AD-A173 590 CONTRIBUTION OF ATMOSPHERIC FORCING TO COOLING OF THE 1/1
ARABIAN SEA DURING ONSET OF THE SOUTHWEST MONSOON(U)
NAVAL POSTGRADUATE SCHOOL MONTEREY CA D W GILLARD
UNCLASSIFIED JUN 86 F/G 8/10 NL

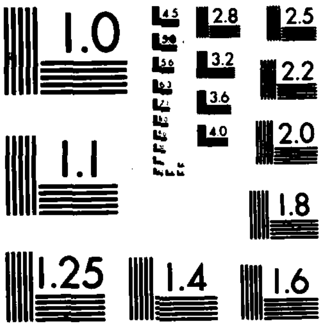
1.0
4.5
5.0
5.6
6.3
2.8
3.2
3.6
4.0
2.5
2.2
2.0
1.1
1.8
1.25
1.4
1.6

ICROCOPY RESOLUTION TEST CHART
NATIONAL BUREAU OF STANDARDS-1963-A

②

AD-A173 590

NAVAL POSTGRADUATE SCHOOL

Monterey, California

DTIC
S ELECTE D
NOV 0 6 1986
D

THESIS

CONTRIBUTION OF ATMOSPHERIC FORCING TO COOLING OF THE ARABIAN SEA DURING ONSET OF THE SOUTHWEST MONSOON

by

David W. Gillard

June 1986

Thesis Advisor: R. L. Elsberry

Approved for public release; distribution unlimited

DTIC FILE COPY

86 11 6 015

AD A 173 590

SECURITY CLASSIFICATION OF THIS PAGE

REPORT DOCUMENTATION PAGE

1a REPORT SECURITY CLASSIFICATION (UNCLASSIFIED)

1b. RESTRICTIVE MARKINGS NONE

2a. SECURITY CLASSIFICATION AUTHORITY

2b. DECLASSIFICATION / DOWNGRADING SCHEDULE

3 DISTRIBUTION / AVAILABILITY OF REPORT
Approved for public release;
distribution unlimited

4 PERFORMING ORGANIZATION REPORT NUMBER(S)

5. MONITORING ORGANIZATION REPORT NUMBER(S)

6a. NAME OF PERFORMING ORGANIZATION Naval Postgraduate School

6b. OFFICE SYMBOL *(If applicable)* 63

7a. NAME OF MONITORING ORGANIZATION Naval Postgraduate School

6c. ADDRESS *(City, State, and ZIP Code)* Monterey, California 93943-5100

7b. ADDRESS *(City, State, and ZIP Code)* Monterey, California 93943-5100

8a. NAME OF FUNDING / SPONSORING ORGANIZATION

8b. OFFICE SYMBOL *(If applicable)*

9. PROCUREMENT INSTRUMENT IDENTIFICATION NUMBER

8c. ADDRESS *(City, State, and ZIP Code)*

10. SOURCE OF FUNDING NUMBERS

PROGRAM ELEMENT NO.	PROJECT NO.	TASK NO.	WORK UNIT ACCESSION NO.

11 TITLE *(Include Security Classification)*
CONTRIBUTION OF ATMOSPHERIC FORCING TO COOLING OF THE ARABIAN SEA DURING ONSET OF THE SOUTHWEST MONSOON

12 PERSONAL AUTHOR(S) Gillard, David W.

13a TYPE OF REPORT Master's Thesis

13b TIME COVERED FROM ________ TO ______

14 DATE OF REPORT *(Year, Month, Day)* 1986 June

15 PAGE COUNT 71

16 SUPPLEMENTARY NOTATION

17 COSATI CODES

FIELD	GROUP	SUB-GROUP

18. SUBJECT TERMS *(Continue on reverse if necessary and identify by block number)*
Atmospheric forcing; mixed layer cooling; Arabian Sea; Garwood ocean mixed layer model; Southwest monsoon onset. (Theses)

19 ABSTRACT *(Continue on reverse if necessary and identify by block number)*

The rapid cooling of the mixed layer in the Arabian Sea during the southwest monsoon onset is examined. The atmospheric forcing fields over the Arabian Sea during the onsets in 1979, 1984 and 1985 are analyzed. Realistic wind speed and evaporative heat flux increases occur soon after onset. The solar radiation flux analyses suggest that both the Navy Operational Global Atmospheric Prediction System and the National Aeronautics and Space Administration four-dimensional data assimilation models are too simplistic for accurate solar radiation flux calculations in the tropics. The solar radiation fluxes appear to be too low during the pre-onset periods and too high during the post-onset periods. The atmospheric forcing fields are then applied to a one-dimensional, ocean mixed layer model at four locations. The magnitude of the predicted sea-surface temperature decrease is 0.5 to 1.0°C during the 1984 and 1985 monsoon onsets. The results suggest that local atmospheric forcing accounts for most of the mixed layer cooling on a time scale of less than ten days and away from any major ocean current regions. The direct heat loss to the atmosphere contributes more to cooling of the mixed layer than does entrainment mixing at the base of the layer.

20 DISTRIBUTION / AVAILABILITY OF ABSTRACT
☒ UNCLASSIFIED/UNLIMITED ☐ SAME AS RPT ☐ DTIC USERS

21 ABSTRACT SECURITY CLASSIFICATION unclassified

22a NAME OF RESPONSIBLE INDIVIDUAL Russell L. Elsberry

22b TELEPHONE *(Include Area Code)* 408-659-2795

22c. OFFICE SYMBOL 63Es

DD FORM 1473, 84 MAR

83 APR edition may be used until exhausted
All other editions are obsolete

SECURITY CLASSIFICATION OF THIS PAGE

Approved for public release; distribution is unlimited.

Contribution of Atmospheric Forcing to Cooling of the Arabian Sea during Onset of the Southwest Monsoon

by

David W. Gillard
Lieutenant, United States Navy
B.S., Purdue University, 1978

Submitted in partial fulfillment of the
requirements for the degree of

MASTER OF SCIENCE IN METEOROLOGY AND OCEANOGRAPHY

from the

NAVAL POSTGRADUATE SCHOOL
June 1986

Author: David W Gillard
David W. Gillard

Approved by: R L Elsberry
R.L. Elsberry, Thesis Advisor

Patrick C Gallacher
P.C. Gallacher, Second Reader

R.J. Renard, Chairman,
Department of Meteorology

JN Dyer
J.N. Dyer,
Dean of Sciences

ABSTRACT

The rapid cooling of the mixed layer in the Arabian Sea during the southwest monsoon onset is examined. The atmospheric forcing fields over the Arabian Sea during the onsets in 1979, 1984 and 1985 are analyzed. Realistic wind speed and evaporative heat flux increases occur soon after onset. The solar radiation flux analyses suggest that both the Navy Operational Global Atmospheric Prediction (NOGAPS) System and the (NASA) National Aeronautics and Space Administration four-dimensional data assimilation models are too simplistic for accurate solar radiation flux calculations in the tropics. The solar radiation fluxes appear to be too low during the pre-onset periods and too high during the post-onset periods. The atmospheric forcing fields are then applied to a one-dimensional, ocean mixed layer model at four locations. The magnitude of the predicted sea-surface temperature decrease is 0.5 to 1.0°C during the 1984 and 1985 monsoon onsets. ~~The~~ results suggest that local atmospheric forcing accounts for most of the mixed layer cooling on a time scale of less than ten days and away from any major ocean current regions. The direct heat loss to the atmosphere contributes more to cooling of the mixed layer than does entrainment mixing at the base of the layer. Keywords: Mixed layer (Marine); →(+ p 1)

QUALITY INSPECTED 4

Accesion For
NTIS CRA&I ☑
DTIC TAB ☐
Unannounced ☐
Justification ....
By ....
Distribution /
Availability Codes
Dist | Avail and / or Special
A-1

TABLE OF CONTENTS

I. INTRODUCTION 9
  A. PURPOSE AND HYPOTHESIS 9
  B. BACKGROUND 9
  C. DATA SOURCES 10
  D. ATMOSPHERIC FORCING OF MIXED LAYER MODEL 11

II. ANALYSES OF ATMOSPHERIC FORCING FIELDS 14
  A. DISCUSSION OF PLAN 14
  B. DATA SOURCES 15
  C. SURFACE FLUXES 16
    1. Solar Radiative Flux 16
    2. Wind Mixing 19
    3. Evaporative Heat Flux 22
    4. Sensible Heat Flux 23
    5. Total (Net) Surface Heat Flux 24
  D. SEA-SURFACE TEMPERATURE FIELDS 25

III. LOCAL FORCING APPLIED TO AN OCEAN MIXED LAYER MODEL 46
  A. THE MODEL 46
  B. MIXED LAYER PREDICTIONS DERIVED FROM THE ATMOSPHERIC FORCING 50

IV. CONCLUSIONS 59
  A. BACKGROUND 59
  B. ATMOSPHERIC FORCING ANALYSIS 59
  C. EXAMINATION OF ATMOSPHERIC FORCING WITH THE MIXED LAYER MODEL 60

APPENDIX A: THE NAVY OPERATIONAL GLOBAL ATMOSPHERIC PREDICTION SYSTEM 63
  1. DYNAMICS 63
  2. MODEL DIABATICS 64

1. Planetary Boundary Layer 64
2. Cumulus Parameterization 65
3. Radiation 65
3. PROBLEMS WITH NOGAPS IN THE TROPICS 65

APPENDIX B: DATA HANDLING PROCEDURES 66
1. ATMOSPHERIC FORCING FIELDS 66
2. MIXED LAYER MODEL DATA 66

LIST OF REFERENCES 67

INITIAL DISTRIBUTION LIST 70

LIST OF TABLES

1. PREVIOUS STUDIES OF ATMOSPHERIC FORCING 12
2. MEAN AND STANDARD DEVIATION OF SOLAR RADIATIVE FLUX, (W/M^2) 17
3. AS IN TABLE 2, EXCEPT FOR AVG. DAILY SOLAR RAD. FLUX. (W/M^2) 18
4. AS IN TABLE 2, EXCEPT FOR ATMOSPHERIC U-MOMENTUM FLUX. (M^2/S^2) 21
5. AS IN TABLE 2, EXCEPT FOR ATMOSPHERIC V-MOMENTUM FLUX. (M^2/S^2) 22
6. AS IN TABLE 2, EXCEPT FOR EVAP. HEAT FLUX. (W/M^2) 23
7. AS IN TABLE 2, BUT FOR SENSIBLE HEAT FLUX. (W/M^2) 24
8. INITIAL CLIMATOLOGICAL TEMPERATURE PROFILE DATA 49
9. RESULTS OF MIXED LAYER PREDICTIONS USING ACTUAL ONSET FORCING 52
10. COMPARISONS OF NOGAPS SST AND MIXED LAYER MODEL PREDICTED SST 53
11. RESULTS OF TESTS OF THE MIXED LAYER PREDICTIONS TO THE ATMOSPHERIC FORCING FIELDS 54

LIST OF FIGURES

1.1 Schematic of mechanisms that effect the mixed layer temperature 13
2.1 Locations of Grid Points 28
2.2 10-day averages of pre-onset and post-onset, solar radiation flux, 1985 29
2.3 Avg. daily solar radiation flux, SW pt., 18 May-4 June, 1985 30
2.4 10-day averages of pre-onset and post-onset, wind speed, 1985 31
2.5 Wind speed, SE pt., 18 May-4 June, 1985 32
2.6 As in Fig. 2.5, but for SW pt. 33
2.7 U-momentum flux, NW pt., 4-21 June, 1979 34
2.8 V-momentum flux, NW pt., 4-21 June, 1979 35
2.9 10-day averages of pre-onset and post-onset, evaporative heat flux, 1985 36
2.10 Evap. heat flux, SW pt., 18 May-4 June, 1985 37
2.11 Evap. heat flux, NW pt., 18 May-4 June, 1985 38
2.12 Sensible heat flux, SW pt., 18 May-4 June, 1985 39
2.13 Total heat flux, SE pt., 18 May-4 June, 1985 40
2.14 As in Fig. 2.13, but for SW pt. 41
2.15 As in Fig. 2.13, but for NE pt. 42
2.16 As in Fig. 2.13, but for NW pt. 43
2.17 SST at all pts., 18 May - 4 June, 1984 44
2.18 As in Fig. 2.18, except for 1985 45
3.1 Climatological and estimated temperature profile at the SE point 56
3.2 Temperatures associated with maximum daily mixed layer depth predicted with actual onset forcing 57
3.3 Maximum daily mixed layer depth predicted with actual onset forcing 57
3.4 Results of sensitivity test of mixed layer predictions : maximum daily temperatures 58
3.5 Results of sensitivity test of mixed layer predictions : maximum daily mixed layer depths 58

ACKNOWLEDGEMENTS

The author would like to thank Mr. Bob Rosenberg at the NASA Goddard Space Flight Center for providing the atmospheric forcing fields for 1979. The data archiving division at Fleet Numerical Oceanography Center provided the atmospheric forcing fields for 1984 and 1985, and Mr. Bob Hale assisted in accessing the data at the Naval Postgraduate School. Dr. Bill Garwood provided the ocean mixed layer prediction model and provided valuable comments on the study. Mr. Mike Clancy and Mr. Ken Pollak at FNOC went to considerable inconvenience to provide the Extended Ocean Thermal System (EOTS) data and also provided helpful comments on the study. Dr. James Boyle provided many hours of assistance in writing the computer codes to read the data tapes. Computer resources were provided by the W.R. Church Computer Center.

Special appreciation is due to Mr. Pat Gallacher who modified the mixed layer model for our use, helped to interpolate atmospheric forcing fields, provided many helpful comments during the project and reviewed the manuscript.

Dr. Russ Elsberry provided the motivation for the study and shaped its progress along the way. His insight into the many aspects of the study and his help in writing the thesis were invaluable. Most of all, the author would like to thank him for his willingness to give of his time and for his encouragement.

Finally, I owe my wife, Joan, my deepest gratitude and love for her patience and support. She is in many ways responsible for the completion of this thesis.

I. *INTRODUCTION*

A. PURPOSE AND HYPOTHESIS

The purpose of this study is to investigate the upper ocean response to atmospheric forcing that is associated with the onset of the southwest monsoon in the Arabian Sea. Estimates of atmospheric surface fluxes as the monsoon begins are then used with the Garwood (1977) one-dimensional bulk mixed layer model to simulate the effects on sea-surface temperature (SST) and mixed layer depth as the monsoon begins. A second objective of this study is to determine which atmospheric forcing parameters can account for the observed cooling of the Arabian Sea immediately following onset of the summer monsoon. The SST decreases rapidly immediately after onset (Krishnamurti, 1981), even though the solar heat flux would be expected to lead to increasing temperatures during this season. The hypothesis of this study is that the increased wind-generated mixing associated with the onset of the monsoon is responsible for the immediate cooling at the ocean surface. This hypothesis is only applicable away from the region of the African coast, where upwelling is likely to be the dominant cooling mechanism, and on the 10-day time scale of monsoon onset.

One motivation for this study is to identify the causes for the Fleet Numerical Oceanography Center (FNOC) upper-ocean model's predictions of excessive cooling of the upper ocean after the southwest monsoon is established (personal communication, M. Clancy, FNOC). Understanding the various ocean cooling mechanisms may contribute to improved predictions and analyses of upper ocean thermal structures in this area. Some studies have also suggested a possible link between SST anomalies in the Arabian Sea after onset and rainfall amounts in India (Babu *et al.* 1985). A better knowledge of the atmospheric forcing that leads to the cooling of the Arabian Sea may then lead to better predictions of rainfall.

B. BACKGROUND

The southwest monsoon over the Arabian Sea occurs annually during late May or early June. It is characterized by a dramatic shift of surface winds from weak easterlies or westerlies to strong southwesterly winds. Krishnamurti *et al.* (1981) found that a tropical cyclone-like feature, termed the onset vortex, accompanies the onset of the monsoon in about 60% of the monsoons observed during a 68-year period. The onset vortex normally forms off the southwest coast of India at about 10°N, 70°E and moves slowly northward and then westward to the Saudi Arabian peninsula area. The strong westerlies to the south of the onset vortex help to establish the southwest monsoon. These monsoonal winds bring rain to the western coast of India and areas northward and inland. In addition to stronger winds, the onset vortex also reduces the solar insolation at the surface due to increased cloud cover. Both of these conditions tend to reduce the SST during the period of the monsoon. Briefly, the mixed layer heat budget is represented by:

$$Q_{ML} = Q_{sfc} + Q_{ent} + Q_{adv} + Q_{upw}, \tag{1.1}$$

where Q_{ML} is the change in heat content in the mixed layer ; Q_{sfc} is the surface heat flux; Q_{ent} is the entrainment heat flux at the base of the layer; Q_{adv} is the heat change due to horizontal advection; and Q_{upw} is the heat flux due to upwelling. These terms are represented in Fig. 1.1. The heat budget is discussed in detail in Chapter II.

Krishnamurti (1981) found that the SST initially decreased by a maximum of 2-3°C in a 5-6 day period soon after the wind strengthened in 1979. He suggested five possible mechanisms for the cooling of the Arabian Sea following onset:

(1) Diminished solar radiation due to increased cloud cover;
(2) Northward flux of heat due to cold oceanic eddies to the north;
(3) Coastal upwelling and downstream shedding of cold eddies;
(4) Strong evaporation in the region of strong winds; and
(5) Strong wind stress-induced upwelling.

This study will also examine the mechanism of turbulent mixing in the upper ocean and the associated entrainment of cooler water from below. Each of these mechanisms are discussed in detail in Chapter II.

C. DATA SOURCES

Two four-dimensional data assimilation models are used as the sources of atmospheric forcing. This type of data is used in place of direct observational analyses to obtain complete and consistent sets of surface fluxes on the space and time scales required for ocean prediction. The observation network in the Arabian Sea is insufficient, even during the First Global atmospheric research program Global Experiment (FGGE), to provide the required data coverage. The data assimilation technique of both data sources is to use predicted fields to fill in the gaps where no observations exist. The National Aeronautics and Space Administration (NASA) four-dimensional data assimilation model is the source of the forcing during 1979. These data were obtained during the FGGE Special Observation Period (SOP) II. The source for 1984 and 1985 is the Navy Operational Global Atmospheric Prediction System (NOGAPS), which is maintained by FNOC. This data source is described in more detail in Appendix A.

Chapter II describes the atmospheric forcing fields from the 1979, 1984 and 1985 summer monsoon seasons. A comparison is made between the atmospheric forcing fields from each data source and interannual differences are noted. The 1979 data should be more accurate since FGGE provided more direct observations, but no concurrent ocean thermal structure data are available to verify the ocean mixed layer predictions. The 1984 and 1985 data are based on fewer observations, but the SST analyses used by NOGAPS are concurrent with the atmospheric forcing. Therefore, data for all three years are analyzed to ascertain the accuracy of each data set in comparison with previous studies listed in Table 1.

D. ATMOSPHERIC FORCING OF MIXED LAYER MODEL

The second part of the study involves the application of the atmospheric forcing parameters to the Garwood ocean mixed layer model. This model assumes no horizontal or vertical advection so that a local heat balance is assumed. It is initialized with climatological temperature and salinity profiles at one meter intervals in the upper 200 m. The model integrates hourly values of net surface heat flux, solar radiative flux and wind stress, and predicts the changes in the mixed layer temperature and depth. Specifically, this study utilizes the predicted maximum daily mixed layer depth and associated temperature, the minimum daily mixed layer depth and associated temperature, and the mean daily mixed layer depth and associated temperature.

A major limitation to this study is the lack of verification SST data. Therefore, the main emphasis will be to determine the relative effects of each forcing mechanism on the mixed layer during monsoon onset.

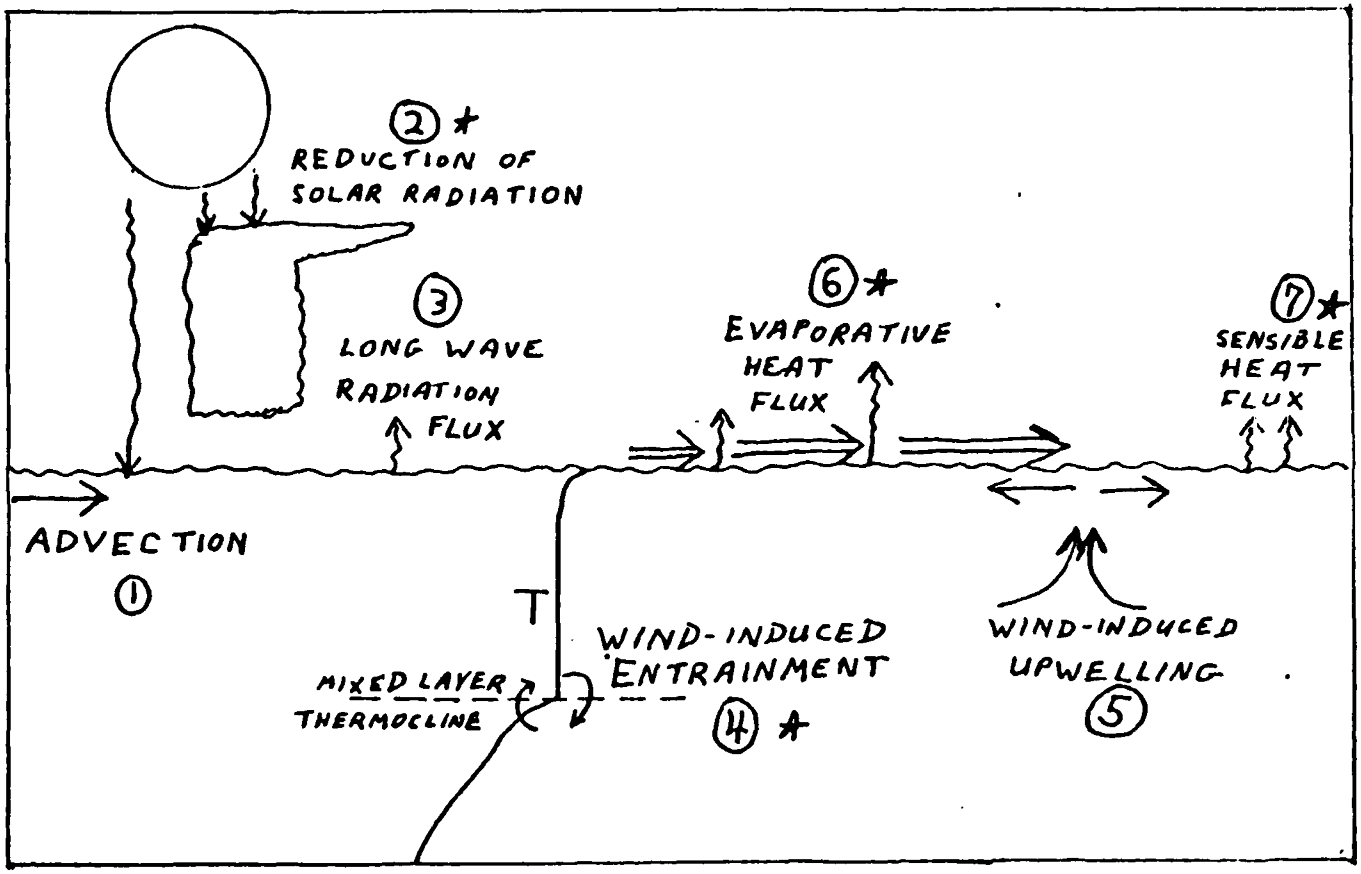
② ★
REDUCTION OF
SOLAR RADIATION
③
LONG WAVE
RADIATION
FLUX
⑥ ★
EVAPORATIVE
HEAT
FLUX
⑦ ★
SENSIBLE
HEAT
FLUX
ADVECTION
①
T
MIXED LAYER
THERMOCLINE
WIND-INDUCED
ENTRAINMENT
④ ★
WIND-INDUCED
UPWELLING
⑤

Fig. 1.1. Schematic illustration of the various mechanisms that can cause cooling of the mixed layer.

II. *ANALYSES OF ATMOSPHERIC FORCING FIELDS*

A. DISCUSSION OF PLAN

This study will address several possible mechanisms that could cause the observed decrease in the SST following onset of the summer monsoon. As previously mentioned, Krishnamurti (1981) suggested five possible mechanisms. Two of the five mechanisms will be discussed and analyzed, along with two other possible causes. These cooling mechanisms include:

(i) Solar radiative flux;
(ii) Wind speed-induced mixing and entrainment;
(iii) Evaporative heat flux; and
(iv) Sensible heat flux.

As Krishnamurti (1981) points out, the northward flux of heat by ocean currents, as estimated by Duing and Leetmaa (1980), is small. Furthermore, this advective heat flux could not respond quickly enough to account for the rapid cooling that occurs after onset. The same argument can be applied to coastal upwelling of cold water. Therefore, advective heat fluxes are not considered in this study. Another mechanism which Krishnamurti considers important for cooling is wind-induced upwelling. Rao (1984) analyzed the depth-time variation of the daily averaged isotherms in the upper 200 meters of the Arabian Sea during the monsoon onset in 1979. After a very strong onset event, the upward velocity of the isotherms is 1 m/day. The heat flux at the base of the mixed layer is:

$$Q(-h) = -c_p \, \rho \, \Delta T dh/dt, \tag{2.1}$$

where Q(-h) is the heat exchange at depth h (the mixed layer depth), c_p is the specific heat of seawater, ρ is the density of seawater, ΔT is the temperature jump across the base of the mixed layer and dh/dt is the vertical velocity of the interface, which is given by:

$$dh/dt = W_{ent} - W_{upw} , \tag{2.2}$$

where W_{ent} is the entrainment velocity and W_{upw} is the upwelling velocity. For a 1°C temperature jump and an upward velocity of 1 m/day, the heat exchange due to upwelling at the base of the mixed layer is approximately 50 W/m^2. This is a small heat flux compared to other fluxes and would not account for the rapid cooling of the mixed layer. The 1°C temperature jump is used in the mixed layer prediction part of the study as a representative value. However, if the temperature jump at the seasonal thermocline was greater, vertical advection would be an important factor in the cooling of the mixed layer. Although vertical advection can be included diagnostically in a one-dimensional mixed layer prediction model (Muller *et al.*, 1984), we neglect vertical and horizontal advection in this study.

B. DATA SOURCES

This study utilizes data provided by the NASA Goddard Space Flight Center for May and June, 1979. The data set was produced from the NASA four-dimensional data assimilation model which uses the previous six-hour prediction field as a first guess for the current analysis field. The archived fields that are relevant for ocean prediction studies include: sensible heat flux, evaporative heat flux, solar radiative flux, and downward fluxes of u-momentum and v-momentum. The assimilation technique produces output four times per day at a grid spacing of 4° latitude x 5° longitude.

This study also uses similar data from the NOGAPS model of FNOC during May and June of 1984 and 1985. This NOGAPS output is also produced four times daily, with analyses at 00 and 12 GMT and six-hour predictions for 06 and 18 GMT. The output fields include: total heat flux, sensible heat flux, evaporative heat flux, solar radiative flux, and zonal and meridional wind speeds. The fields are on a 73 x 144 grid with 2.5° latitude x 2.5° longitude spacing.

These data are analyzed in three ways. A 10-day average is computed for the pre-onset period on a grid centered on the Arabian Sea, bounded by the equator, 25°N, 50°E and 75°E (Fig. 2.1). The pre-onset period for 1979 is 5 - 14 June. The actual onset occurred during 16 - 18 June. The pre-onset period for 1984 and 1985 is 15 - 24 May and 17 - 26 May, respectively. The onset occurred during 26 - 28 May for both 1984 and 1985. A 10-day average is also computed for the post-onset periods in all three years: 20 - 29 June 1979 and 3 - 12 June in both 1984 and 1985. Standard deviations from these average values for the pre-onset and post-onset periods are also calculated to provide a measure of the time variability of the atmospheric forcing.

The third analysis method is a time series of all the atmospheric forcing fields centered on the onset date. The time series are examined for four points in the Arabian Sea (Fig. 2.1) that are located well away from any currents. The northwest point (NW) is at 15°N, 57.5°E; the northeast point (NE) is at 15°N, 67.5°E; the southeast point (SE) is at 5°N, 67.5°E; and the southwest point (SW) is at 5°N, 57.5°E. These data fields will be compared with similar data from other studies for the purpose of characterizing the monsoon onset events of 1979, 1984 and 1985 and to verify the suitability of the atmospheric forcing for ocean prediction studies.

C. SURFACE FLUXES

The heat budget equation at the sea surface is:

$$Q_T = Q_b - Q_i + Q_e + Q_s , \tag{2.3}$$

where Q_T is the total heat flux from ocean to atmosphere; Q_b is the net flux of long-wave radiation; Q_i is the downward flux of solar radiation; Q_e is the upward flux of evaporative (latent) heat; and Q_s is the sensible heat flux. The Q_b term is not explicitly analyzed in this study. It can be computed as a residual from the remaining terms. The long-wave radiation flux actually decreases slightly after onset because of increased cloud cover, but the magnitude of the long-wave radiation flux is small and it is not a major factor in the heat budget. These heat fluxes are summarized in the following sections, based on the studies in Table 1.

1. *Solar Radiative Flux*

This flux is a major source of heating prior to onset. The zenith angle of the sun is very low, approximately 10° on May 15 at 10°N, and the sky is generally clear with high optical transmissivity. Gautier (1986) describes how the solar radiative flux decreases sharply as the monsoon onset begins. She illustrates the formation and northward migration of the Maximum Cloudiness Zone (MCZ) in June, 1979. The MCZ clearly follows the path of the onset vortex that is traced in Krishnamurti *et al.* (1981) and Rao (1984). For the Arabian Sea, a typical value of daily net short wave radiative flux before onset is 300 W/m^2. After onset, typical flux values decrease to about 250 W/m^2 with minimum values of 75 W/m^2 under the MCZ. Krishnamurti (1981) indicates that the rapid cooling of the Arabian Sea is generally not attributed to this effect, because the heat capacity of the ocean causes a lag time of one to two months in response to solar radiation. Nonetheless, solar radiative flux is an important component of the energy balance equation as will be shown in the simulations with the Garwood mixed-layer model.

The solar radiative flux values are available each six-hour from the NASA and NOGAPS analyses. This time interval is insufficient to indicate the true maximum solar radiation as a function of time. Therefore, an interpolation scheme (Gallacher, 1979) is used to calculate hourly values from these six-hour values. The pre-onset and post-onset solar radiative fluxes at 12 GMT at the four points are listed in Table 2 for 1979, 1984 and 1985.

TABLE 2

MEAN AND STANDARD DEVIATION OF SOLAR RADIATIVE FLUX, (W/M^2)

	1979		1984		1985	
Pre-onset	873 (208)	918 (23)	313 (5)	246 (35)	355 (3)	306 (23)
	415 (200)	346 (205)	287 (20)	206 (18)	280 (10)	202 (24)
Post-onset	653 (247)	483 (256)	338 (13)	230 (12)	312 (58)	233 (16)
	693 (288)	527 (282)	340 (10)	197 (3)	311 (24)	210 (10)

Data are organized by year, time period, location and whether mean or (standard deviation). For example, in the 1979 pre-onset period, the mean fluxes at the NW, NE, SE and SW points are 873, 918, 346 and 415 W/m^2, respectively.

The solar flux values are generally greater to the north during the northern summer at these latitudes, and they are greater to the west where 12 GMT lies closer to local noon. The 1979 (NASA model) solar flux values appear to be phase-shifted as the 12 GMT values are larger than the 06 GMT values (not shown). By contrast, the western values in the other years (FNOC model) are larger than the eastern values. The nature and reason for the phase difference has not been determined in this study. Note the comparison between values in the pre-onset and post-onset periods. The 10-day mean values at the northern points are representative of cloudier conditions between the solar fluxes in the two periods. As shown in Fig. 2.3, the time series of average daily solar radiative flux at the SW point from 18 May to 4 June 1985 indicates only a slight decrease of daily solar radiative flux. This is also true at the other points in 1984 and 1985. In 1979, when an onset vortex is well documented in various studies, the average daily solar radiative flux at the northern points decreases more than in the other years (Table 3) during the period of onset. This supports the findings of Gautier (1986). It is possible that the MCZ in 1984 and 1985 simply did not cross over the geographical points that were selected. A more likely possibility is that NOGAPS does not properly calculate the effect of cloudiness on solar radiative flux (see Appendix A). In any case, it is unlikely that the increased cloudiness would decrease the solar flux over enough area and a sufficiently long time to cause an appreciable cooling at the surface. Therefore, the solar radiative flux is not likely to be a major cause of the observed SST decrease.

2. *Wind Mixing*

Several studies have indicated that increased wind stress should induce mixing and entrainment at the base of the mixed layer. Ramanadham *et al.* (1981) illustrates the wind increase at four points in the Arabian Sea during June 1977. The largest wind increase is from 3 to 8 m/s in 1 - 2 days at 10.5°N, 66°E. Krishnamurti (1981) shows an even stronger increase in wind speed at 7°N, 66°E during the onset of the monsoon in 1979, from approximately 4 m/s to 13 m/s in 1 - 2 days.

The mixed layer warms and shallows prior to the monsoon onset as a result of light winds and strong insolation. Rao *et al.* (1981) examine the variability of the mixed layer in the area of the central Arabian Sea during the southwest monsoon in 1977. The mixed layer depth (MLD) is at approximately 40 m prior to onset in May and June. During the onset phase, the MLD increases to 70 m in two weeks and deepens further as the monsoon progresses. The mean temperature of the mixed layer cools by 1°C within one week after onset. Rao *et al.* (1981) attribute this deepening and cooling primarily to wind mixing and also to the convective overturning caused by upward heat flux at the surface. It is the hypothesis of this study that the increased wind stress at the sea-surface mixes the surface layer and entrains cooler water from below the base of the mixed layer, which simultaneously deepens and cools the layer.

The zonal and meridional components of the wind are extracted from the NOGAPS analyses. The southwest monsoonal winds generally show very little variation in direction after onset, so the variability is primarily in wind speed. The calculation of wind stress, τ, is described in Chapter III. Finally, the downward fluxes of u-momentum ($u'w'$) and v-momentum ($v'w'$) are computed by dividing the wind stress components by the air density, ρ. These fluxes of momentum are used to compare with the momentum fluxes which have been extracted directly from the NASA analysis for 1979. Wind stress values are used as atmospheric forcing inputs to the Garwood mixed layer prediction model.

Table 4 lists means and standard deviations for the u-momentum flux. Negative values indicate a downward flux of westerly momentum since w is negative in the downward direction. Notice the large increase in westerly momentum flux in the post-onset period for most of the points. Some exceptions are the momentum fluxes at the SW and SE points in 1985 which are less in the post-onset period than in the pre-onset period. This can be explained by noting that the wind speed at those points is stronger after onset (see Fig. 2.4a) than before onset (see Fig. 2.4b), but the westerly component of the wind is less. Notice also that the standard deviations are generally larger for 1979 than for 1984 or 1985. Since the data for 1979 were obtained as part of FGGE SOP II, it is likely that the greater number of observations contributes to the larger standard deviations in 1979, whereas the NOGAPS analyses are smoother with smaller standard deviations. However, some of these interannual differences may be due to the natural variability in the monsoon, because the 1979 monsoon does seem to have stronger winds overall.

Table 5 lists similar calculations for the v-momentum flux. Negative values indicate a downward flux of southerly momentum. These mean values are generally less than the corresponding values in Table 4 because the monsoonal winds are predominantly westerly, especially after onset. The post-onset periods again have significantly higher values of momentum flux than do the pre-onset periods. In particular, the v-momentum fluxes increase sharply in 1979. The onset vortex that has already been discussed is responsible for these effects. It is obvious from these two tables that the monsoon onset is accompanied by a major increase in surface wind stress, which will enhance turbulent mixing in the ocean.

TABLE 5

AS IN TABLE 2, EXCEPT FOR ATMOSPHERIC V-MOMENTUM FLUX. (M^2/S^2)

	1979		1984		1985	
Pre-onset	-0.05 (0.08)	-0.01 (0.03)	0.00 (0.01)	+0.04 (0.04)	0.00 (0.01)	+0.01 (0.01)
	-0.04 (0.08)	-0.02 (0.03)	-0.02 (0.02)	-0.02 (0.04)	-0.02 (0.02)	-0.01 (0.02)
Post-onset	-0.50 (0.22)	-0.32 (0.24)	-0.02 (0.03)	+0.02 (0.04)	-0.05 (0.07)	-0.01 (0.02)
	0.00 (0.07)	-0.02 (0.07)	-0.09 (0.04)	-0.02 (0.02)	-0.08 (0.04)	0.00 (0.01)

3. *Evaporative Heat Flux*

Ramanadham *et al.* (1981) show that the evaporative heat flux is highly correlated with wind speed, with increases to about 260 W/m^2 as the monsoon winds increase and values of about 150 W/m^2 when the winds subside. Krishnamurti (1981) lists this flux as possibly being an important factor in cooling the sea surface.

Table 6 is a compilation of the 10-day mean values and standard deviations of evaporative heat flux for the four points during the pre- and post-onset periods of 1979, 1984 and 1985. The mean values are comparable for all three years, but the standard deviations of the 1979 (NASA) data are generally significantly higher than in 1984 and 1985 (FNOC). Also, the mean values for the northern points in the post-onset period are approximately twice as large as the pre-onset values. The fluxes at the southern points do not increase significantly (and sometimes decrease) following onset. This follows a similar trend in wind speed and wind stress at these locations.

Figs. 2.9a and 2.9b illustrate the distribution of the evaporative heat flux in 1985 before and after onset, respectively. Notice the spread of the area of maximum flux across the central Arabian Sea after onset. Examples of the evaporative heat flux increasing with time at the SW and NW points during 1985 are shown in Figs. 2.10

TABLE 6

AS IN TABLE 2, EXCEPT FOR EVAP. HEAT FLUX. (W/M^2)

	1979		1984		1985	
Pre-onset	132 (80)	91 (71)	112 (1)	222 (18)	161 (18)	132 (1)
	151 (49)	120 (58)	381 (17)	339 (9)	342 (50)	277 (3)
Post-onset	230 (82)	170 (62)	295 (18)	350 (28)	379 (9)	321 (33)
	189 (41)	160 (84)	382 (7)	224 (0)	405 (29)	229 (25)

and 2.11. The evaporative heat flux increases sharply from about 300 W/M^2 to 700 W/M^2 from 26 to 28 May at the SW point, but it increases by only about 150 W/M^2 from 26 May to 3 June at the NW point. This points out that the low-level jet is a very localized feature that may not affect all locations equally.

4. *Sensible Heat Flux*

Ramanadham *et al.* (1981) analyze the sensible heat fluxes over the eastern Arabian Sea during June 1977. The magnitude of the sensible heat flux typically is on the order of 10 - 50 W/m^2, and is higher at the time of onset when the wind speed is greatest. Krishnamurti and Ramanathan (1982) point out that the Bowen ratio, expressed as sensible heat flux/evaporative heat flux, is typically on the order of 0.01 in the tropics. The Bowen ratio in the study by Ramanadham *et al.* (1981) is approximately 0.1.

The 10-day average Bowen ratio at the SW point at 12 GMT is 120/600 = 0.2, which indicates the relative importance of the evaporative heat flux over the sensible heat flux. This confirms that sensible heat flux has a relatively small influence on tropical ocean cooling during the monsoon onset.

Table 7 lists the mean values and standard deviations of the instantaneous 12 GMT sensible heat flux values for the NASA and NOGAPS data. Positive values indicate sensible heat flux from the ocean to the atmosphere. The mean values of flux are all positive and have small magnitudes. They do not show a large increase from the pre-onset period to the post-onset period. The NASA data for 1979 again have higher standard deviations than do the NOGAPS data for 1984 and 1985.

TABLE 7

AS IN TABLE 2, BUT FOR SENSIBLE HEAT FLUX. (W/M^2)

	1979		1984		1985	
Pre-onset	17 (16)	7 (8)	20 (10)	57 (9)	43 (7)	20 (4)
	28 (14)	22 (10)	58 (1)	55 (0)	57 (6)	32 (3)
Post-onset	27 (22)	13 (22)	38 (21)	55 (9)	17 (7)	44 (11)
	25 (9)	15 (11)	71 (8)	43 (1)	61 (3)	48 (8)

A typical time series of sensible heat flux is given in Fig. 2.12 at the SW point in 1985. The sensible heat flux increases significantly during the onset period. The average magnitude of the flux is about 50 W/m^2 before onset (27 May) and about 120 W/m^2 shortly after onset (30 May). This increase is larger than Ramanadham *et al.* (1981) found, but still is small compared to the evaporative heat flux discussed earlier. Sensible heat flux is therefore not expected to be primarily responsible for the observed cooling.

5. *Total (Net) Surface Heat Flux*

The total heat flux is the sum of the three heat fluxes discussed above plus the downward solar radiative flux plus the net flux of long-wave radiation. Since the total heat flux is extracted from the NOGAPS atmospheric prediction model, the outgoing radiative flux can be calculated from the remaining terms. This study does not consider the long-wave radiation flux for analysis.

Ramanadham *et al.* (1981) indicate the total heat flux from ocean to atmosphere increases very slightly as the onset begins, and decreases strongly as the evaporative and sensible heat fluxes decrease after onset. However, the onset in 1977 appears to be somewhat anomalous compared to the values in this study. The NOGAPS total heat flux fields for 1985 show an increase in the daily mean heat flux of 350 - 400 W/m^2 from the pre-onset to the post-onset periods at the SE and SW points (see Fig. 2.13 and Fig. 2.14). Positive values indicate a flux of heat from the ocean to the atmosphere. The strong diurnal variation of the total heat flux is obvious in these figures. The solar radiation during the day forces the total heat flux to be negative (into the ocean), but at night the flux is to the atmosphere. As has been indicated, the SW point is affected more strongly by the onset and the total heat flux increases more at this point than at the SE point. These flux increases are consistent with the previous analyses of the component heat fluxes. The evaporative heat flux is the dominant component and is responsible for most of the increase in total heat flux. The two northern points show a smaller increase of approximately 150 - 200 W/m^2 (see Fig. 2.15 and Fig. 2.16). The corresponding total heat flux increases in 1984 (not shown) are only about half as large, which indicates a more gradual or less intense monsoon onset.

D. SEA-SURFACE TEMPERATURE FIELDS

Several studies have analyzed SST changes during the onset phase of the monsoon in the Arabian Sea. The SST at 7°N, 66°E decreases from 30°C to 27.5°C in a 6-day period during 1979 as the wind increases from 4 to 14 m/s (Krishnamurti, 1981). Ramanadham *et al.* (1981) indicate that the SST decreases at various points in the Arabian Sea during 1977 are on the order of 0.5°C. The heat fluxes and wind speeds in that study indicate that the onset was not dramatic, which explains the smaller decreases in SST during 1977.

The NOGAPS SST data are produced from a mix of observations, climatology and an ocean model called the Thermal Ocean Prediction System (TOPS). The first-guess field for the SST analysis is the previous 12-hour prediction (Clancy and Pollack, 1983). In the absence of new observations, the new analysis will simply be the first-guess field from TOPS with a small correction toward climatology. The NASA data set available to us does not include the SST field in 1979.

The time series of SST for all four geographical points during 1984 and 1985 are given in Figs. 2.17 and 2.18, respectively. In 1984, the SST at the NW point decreases

0.5°C in 4 - 5 days starting 1 June, whereas the SST at the NE point increases and then decreases during the period. A stepwise decrease of 0.6°C occurs at the SE point during the 18-day period. The SST decreases a total of 1.0°C steadily through the entire period at the SW point in 1984. In 1985, the NW point has a steady decrease of 1.0°C after 19 May. A constant SST is found at the NE point until 26 May 1985 when a brief increase occurs and then a moderate decrease follows. The SW point similarly shows a modest decrease of 0.5°C in 9 days after 26 May 1985. A more dramatic decrease in SST of nearly 1°C in 8 - 9 days starts 29 May 1985 at the SE point.

The SST fields used by the NOGAPS analyses show a cooling trend at the NW, SW and SE points over the 18-day period around the onset in 1984 and in 1985. The time and rate of decrease varies from point to point and year to year. The decrease in the sea-surface temperature is not as great in 1984 or 1985 as Krishnamurti (1981) reports in 1979. Only the decrease of 1°C in 8 - 9 days at the SW point in 1985 approaches the significant cooling event of 1979. No onset vortex occurred during 1985. The monsoon onset of 1979 evidently was not typical in strength or timing. In both 1984 and 1985, the SST decreases during onset at all the points except for the NE point. Several possibilities exist to explain this anomaly:

1. The NE point is not affected by the onset as much. However, the atmospheric forcing analyses do not support this statement. The onset appears to be more intense than at the NW point where the SST decreases.
2. The cumulus parameterization and solar radiation flux calculations are inaccurate. This may be partially correct, but again, the NW point should show similar results and does not.
3. The initial mixed layer temperature and depth are more resistant to onset cooling. This is a factor that cannot be verified in this study because we have no verification mixed layer data.
4. The TOPS model does not parameterize the solar absorption in the mixed layer correctly. Again, this possibility can only be proven if verification mixed layer data are used.

The reason for the differences in the NE point SST field remains unanswered in this study, but the solution would be useful for mixed layer simulations in this area.

Which of the atmospheric forcing fields are responsible for the observed SST cooling? Much of the following discussion will focus on the large cooling which is observed at the SE point in 1985. From the atmospheric forcing analysis, only two mechanisms appear to be significant factors in causing the SST decrease: evaporative heat flux and wind speed or stress. Comparing Figs. 2.10 and 2.6, the wind speed and evaporative heat flux curves increase and decrease together in time and magnitude.

Increased evaporative heat flux causes cooling at the surface and increased wind stress causes cooling by entrainment at the base of the layer. The Garwood ocean mixed layer model will be used to demonstrate the resulting effect on SST by varying these atmospheric forcing parameters.

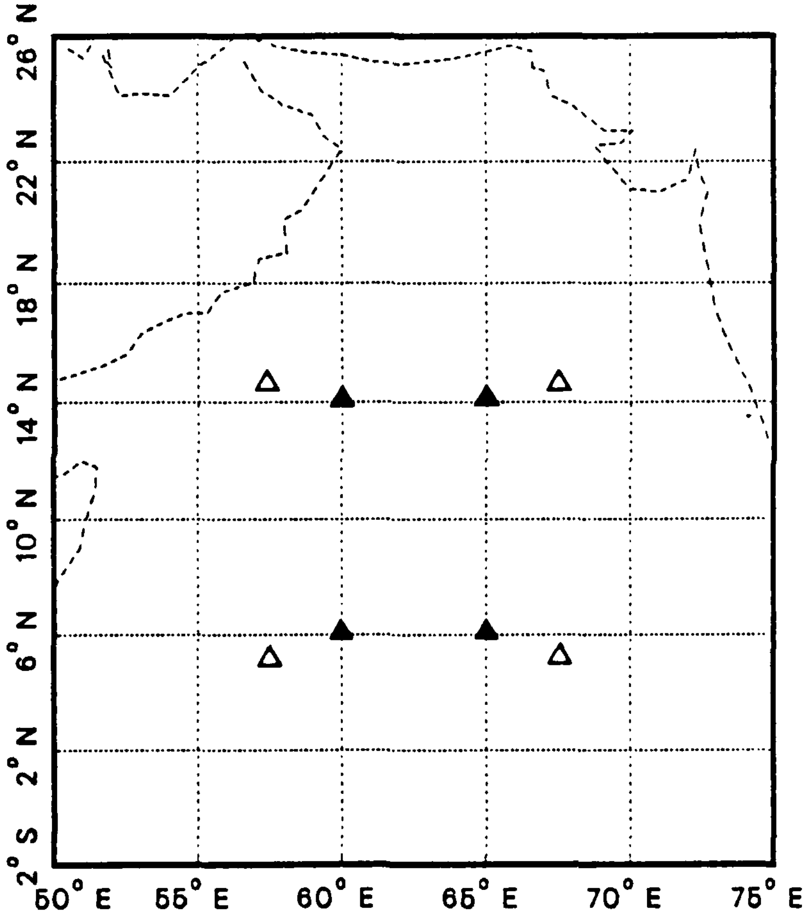
26° N
22° N
18° N
14° N
10° N
6° N
2° N
2° S
50° E
55° E
60° E
65° E
70° E
75° E

Fig. 2.1. Locations of grid points in the Arabian Sea. NOGAPS anaysis points: △ . NASA analysis points: ▲ .

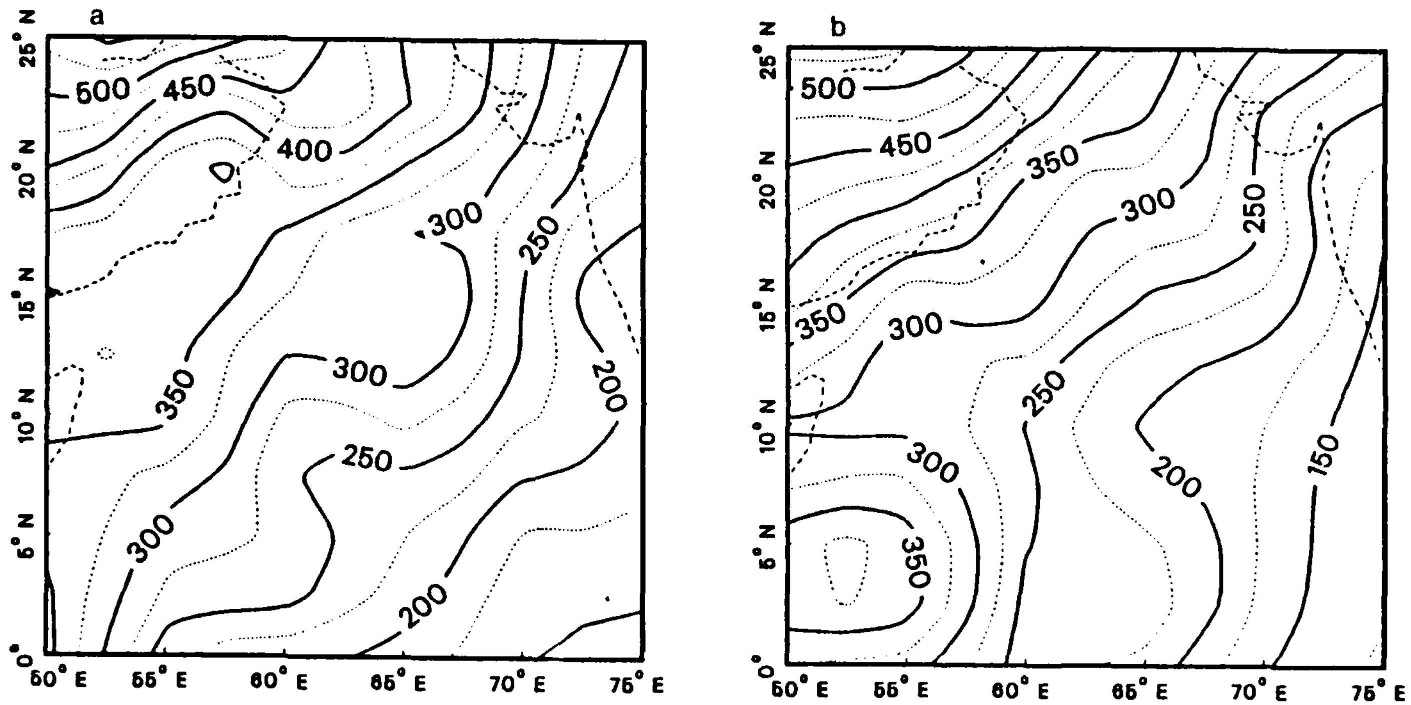
a
b
500
450
400
350
300
250
200
150
25° N
20° N
15° N
10° N
5° N
0°
50° E
55° E
60° E
65° E
70° E
75° E

Fig. 2.2. 10-day averages of solar radiation flux (W/m^2) at 12 GMT in 1985. (a) Pre-onset period (17-26 May). (b) Post-onset period (3-12 June).

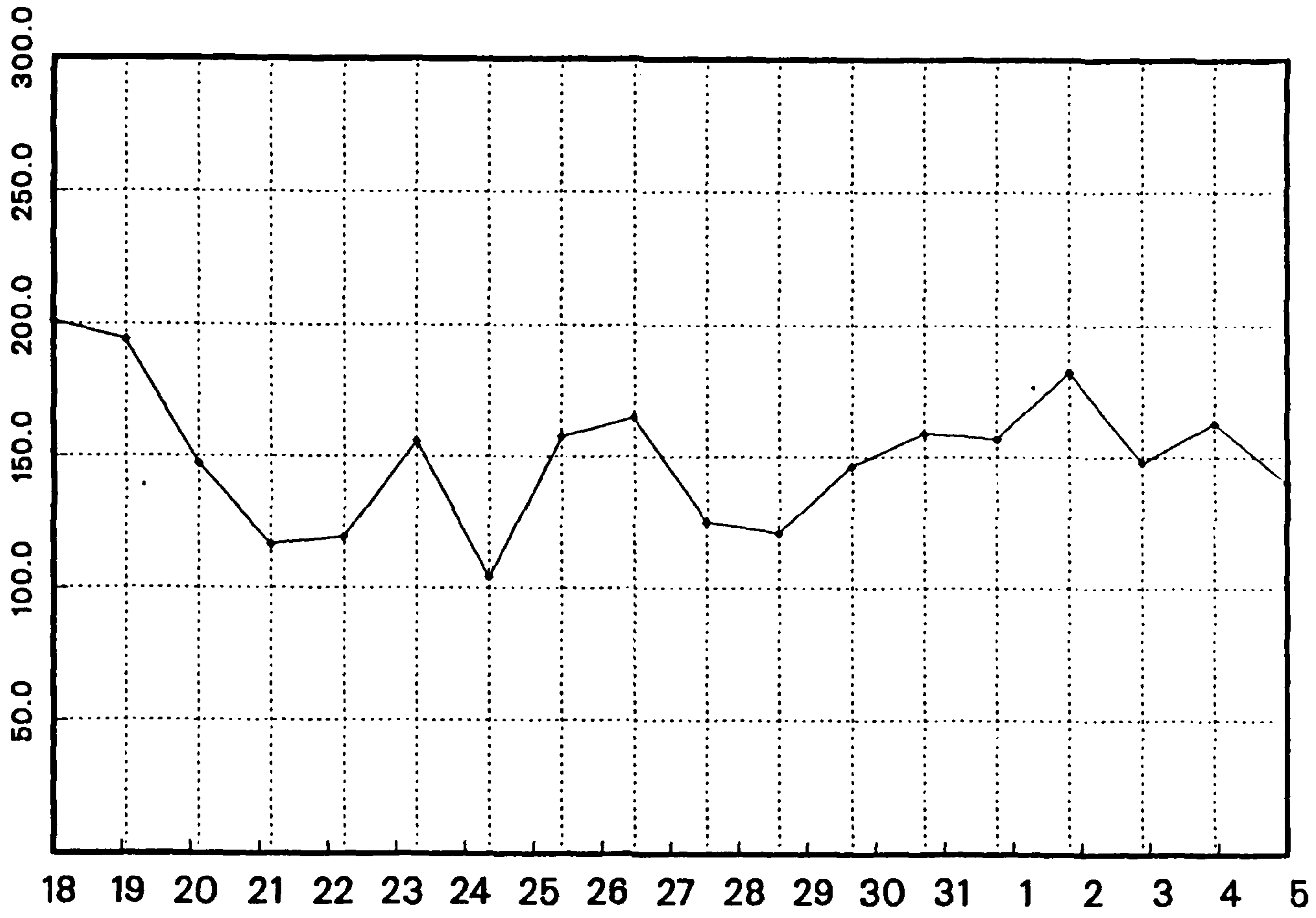

Fig. 2.3. Average daily solar radiation flux (W/m^2) at the SW point during the onset in 1985 (18 May-4 June). Date of onset is ~27 May.

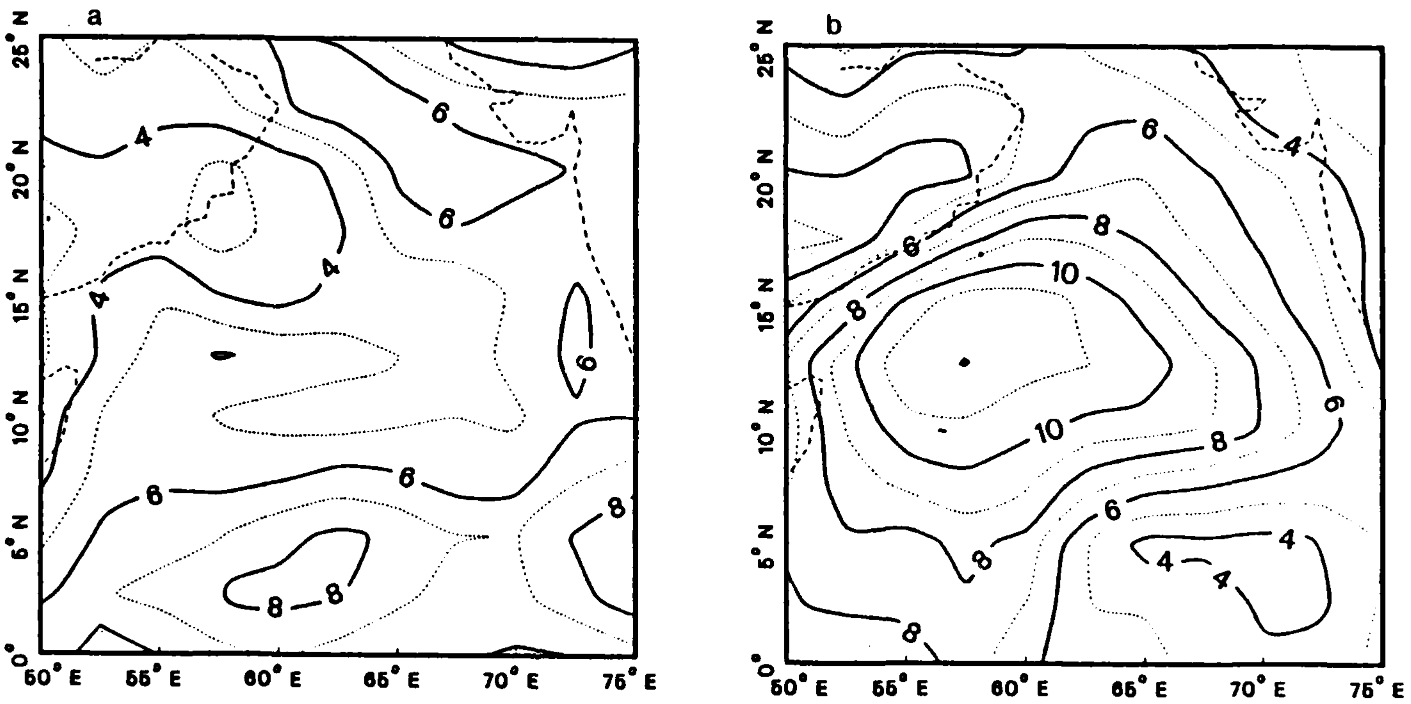
a
25° N
20° N
15° N
10° N
5° N
0°
50° E
55° E
60° E
65° E
70° E
75° E
4
4
4
6
6
6
6
6
8
8
8
b
25° N
20° N
15° N
10° N
5° N
0°
50° E
55° E
60° E
65° E
70° E
75° E
4
4
4
4
6
6
6
6
8
8
8
8
8
10
10

Fig. 2.4. 10-day averages of the wind speed (m/s) at 12 GMT in 1985. (a) Pre-onset period (17-26 May); (b) Post-onset period (3-12 June).

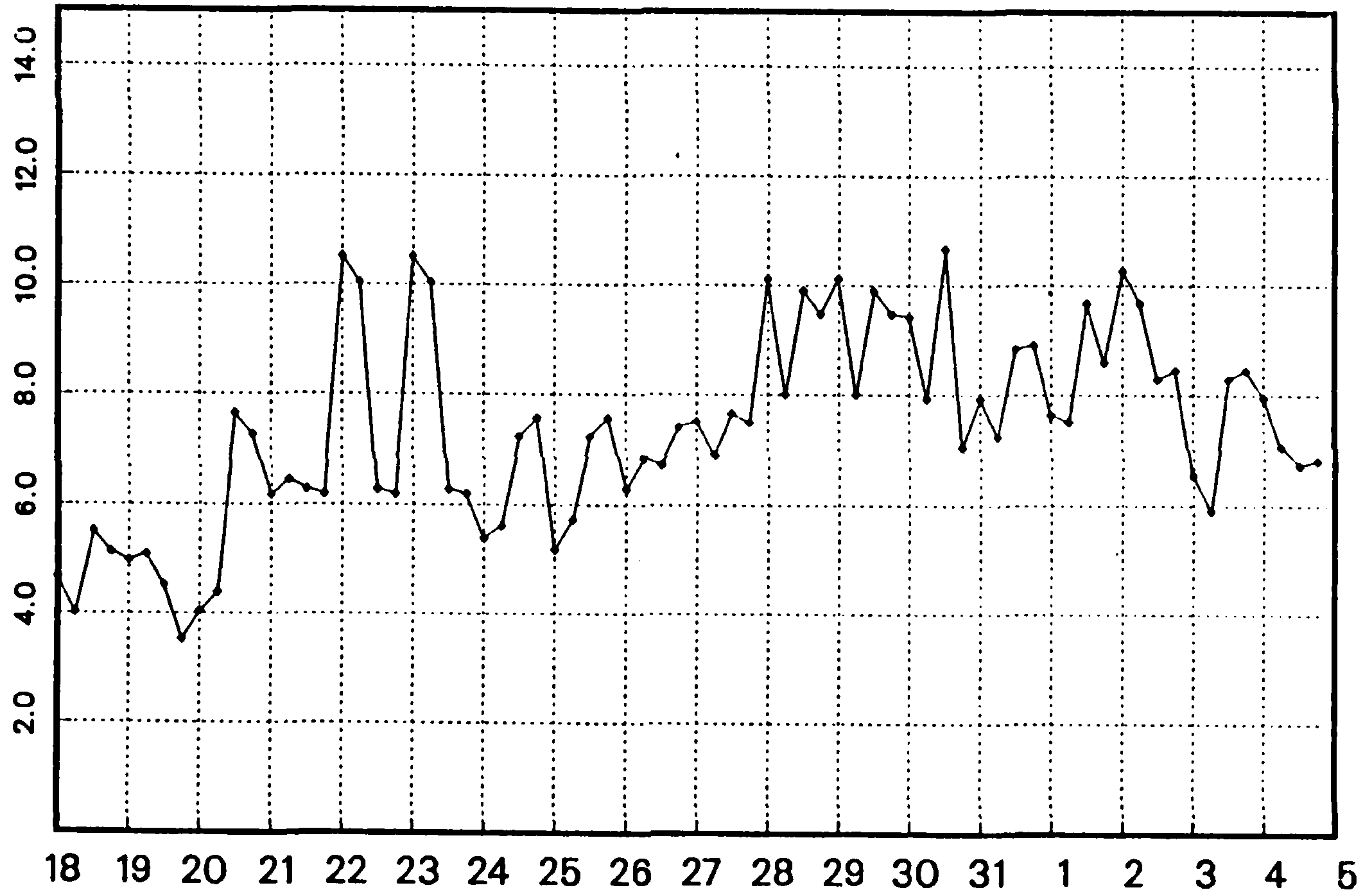

Fig. 2.5. Wind speed (m/s) at the SE point during the onset in 1985 (18 May-4 June). Date of onset is ~27 May. Values are plotted every 6 hours.

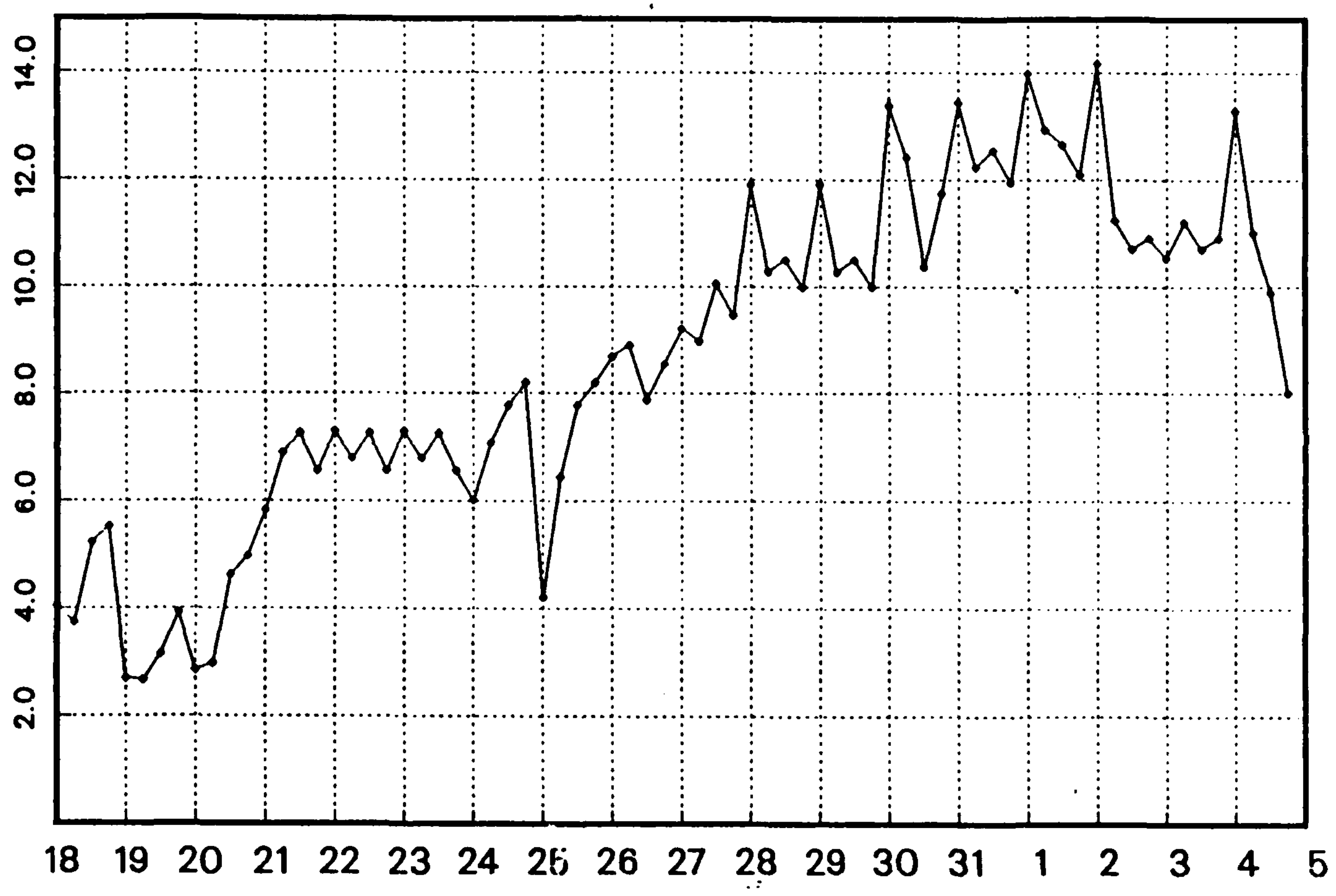

Fig. 2.6. As in Fig. 2.5, except for the SW point.

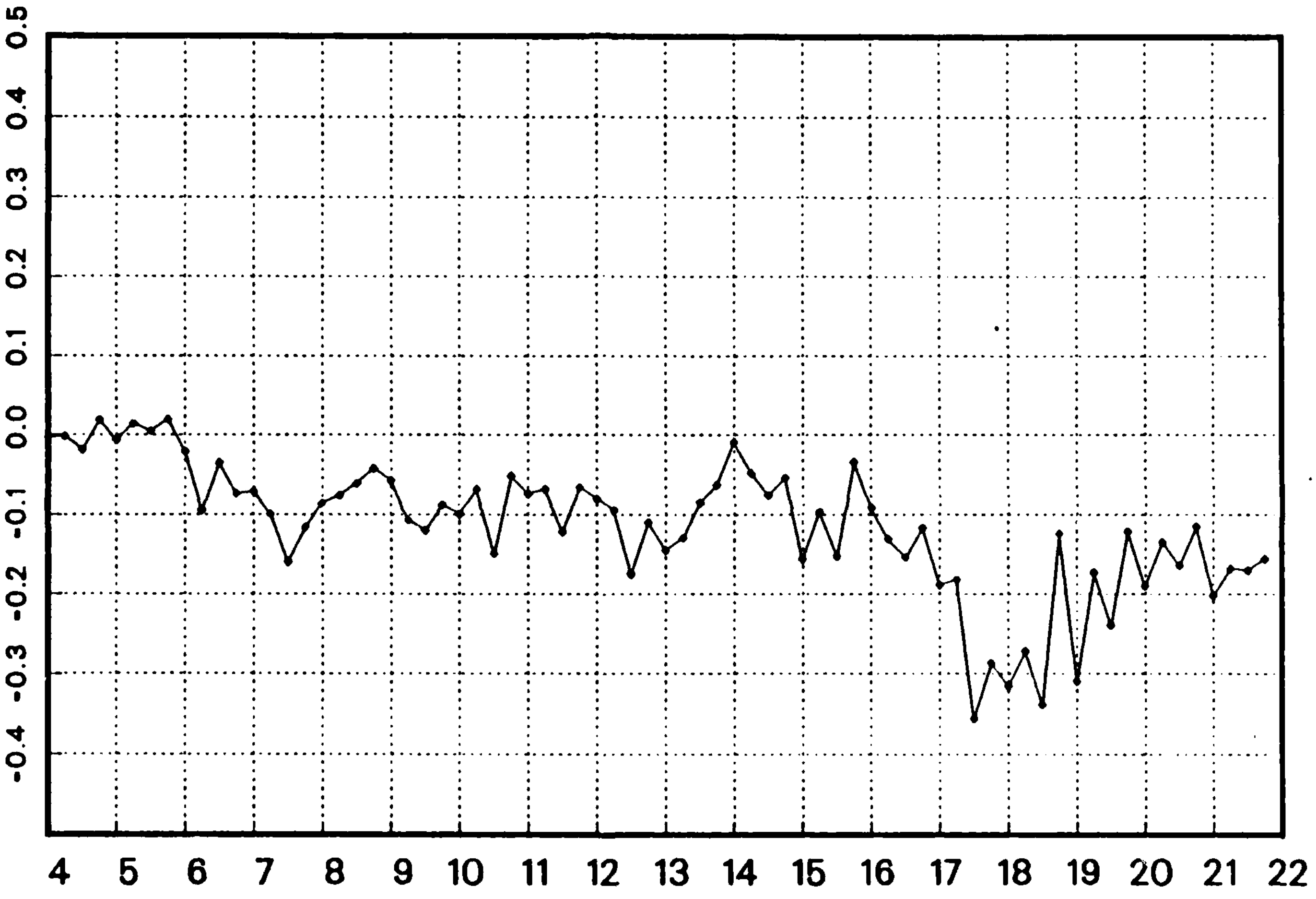

Fig. 2.7. U-momentum flux (m^2/s^2) at the NW point during the onset in 1979 (4-22 June). Date of onset is ~17 June. Negative values indicate momentum flux to the east. Values are plotted every 6 hours.

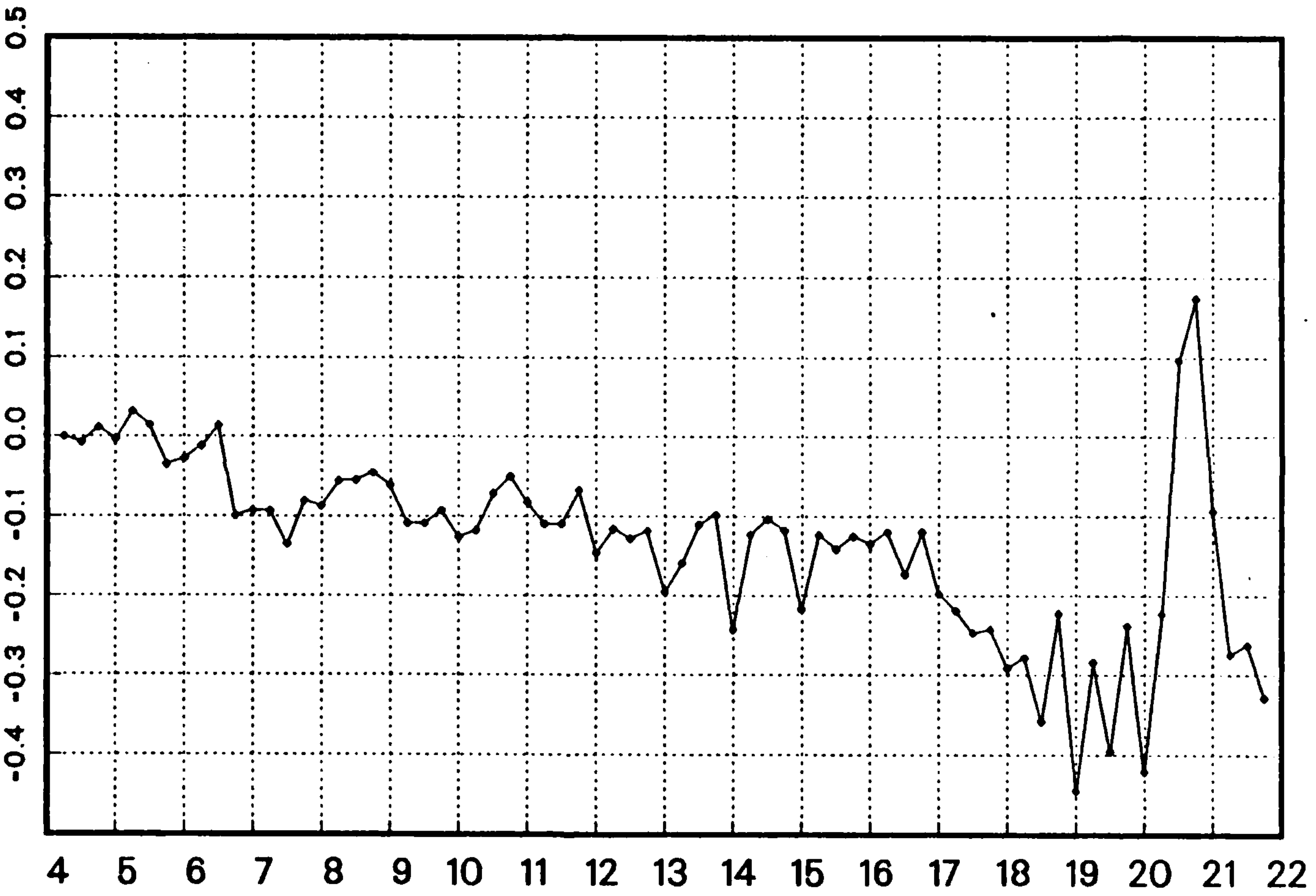

Fig. 2.8. V-momentum flux (m^2/s^2) at the NW point during the onset in 1979 (4-22 June). Date of onset is ~17 June. Negative values indicate momentum flux to the south. Values are plotted every 6 hours.

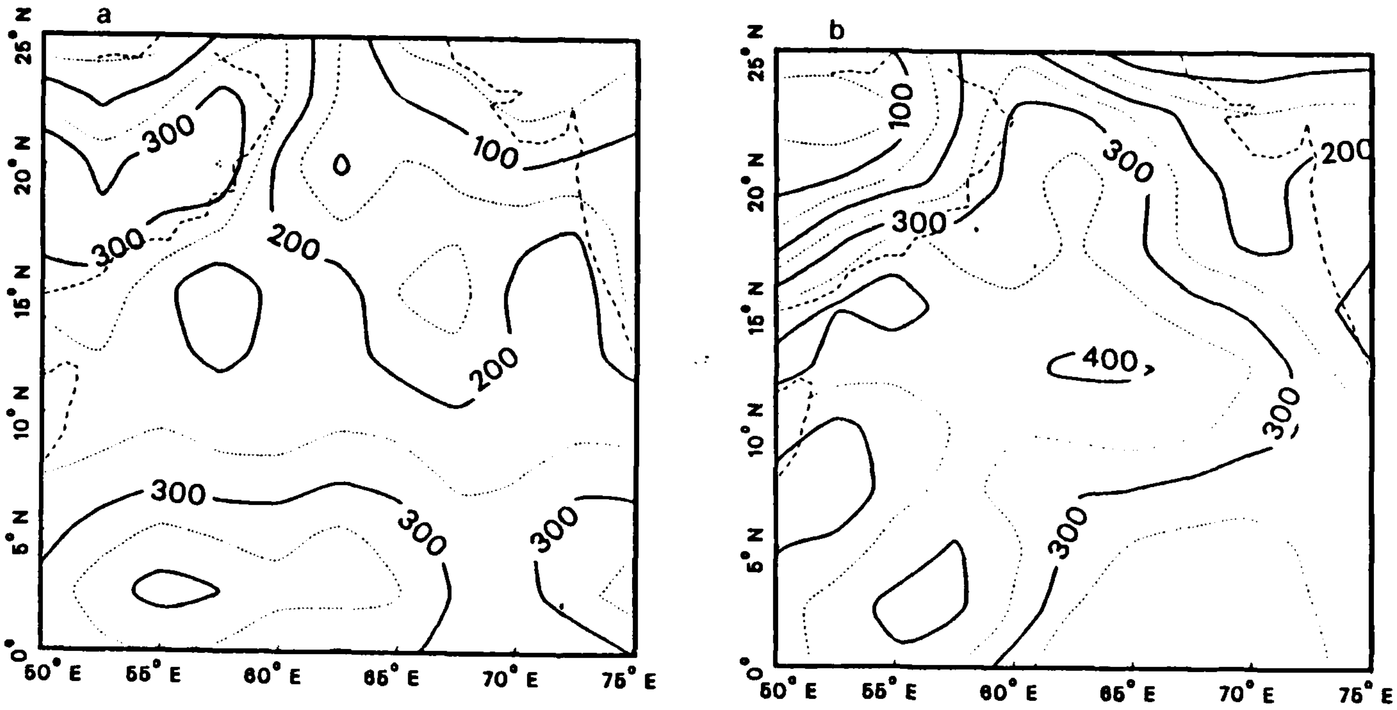
a
b
25° N
20° N
15° N
10° N
5° N
0°
50° E
55° E
60° E
65° E
70° E
75° E
300
300
0
100
200
200
300
300
300
100
300
300
200
400
300
300

Fig. 2.9. 10-day averages of evaporative heat flux (W/m²) at 12 GMT in 1985. (a) Pre-onset period (17-26 May). (b) Post-onset period (3-12 June).

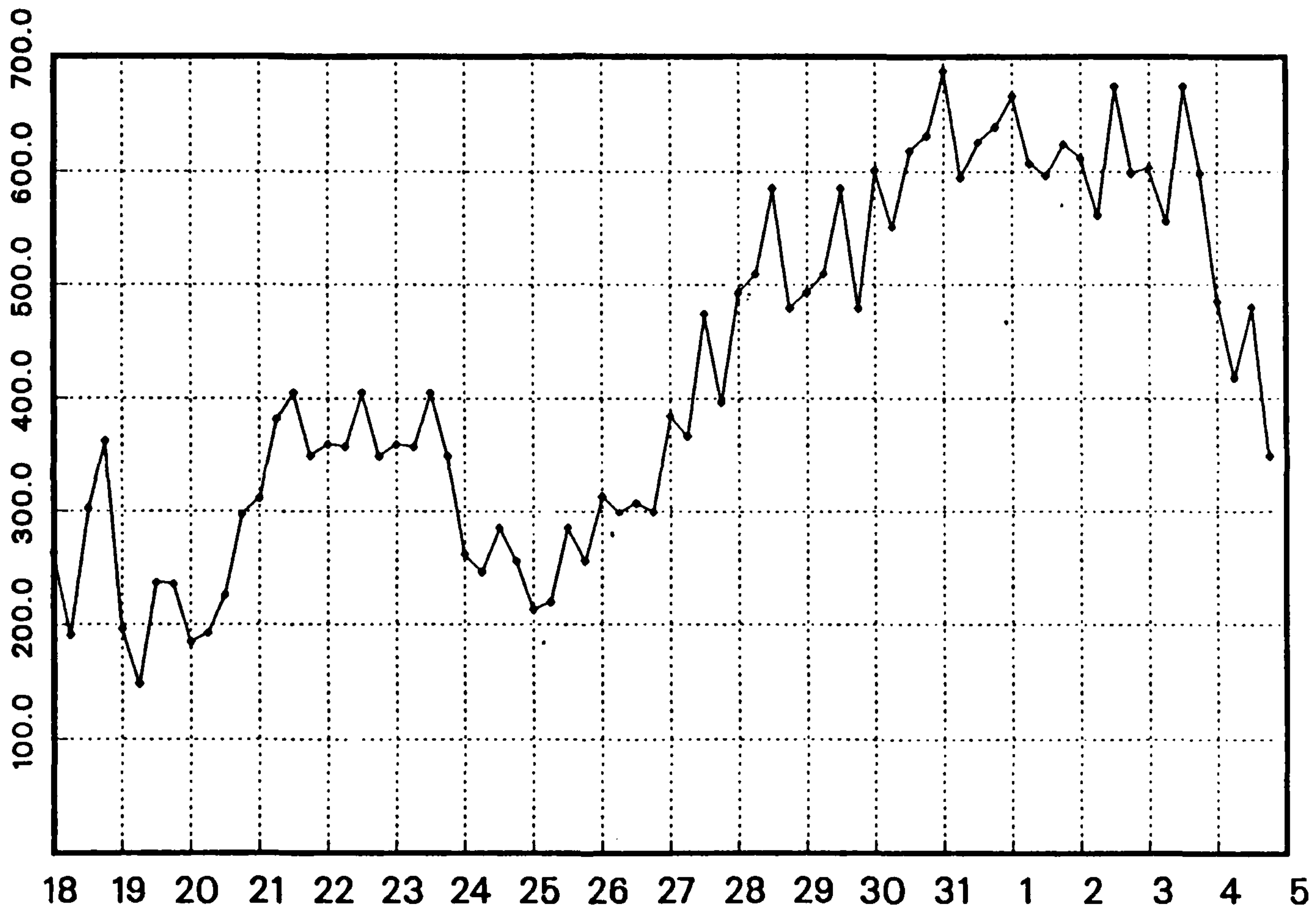

Fig. 2.10. Evaporative heat flux (W/m^2) at the SW point during the onset in 1985 (18 May-4 June). Date of onset is ~27 May. Values are plotted every 6 hours.

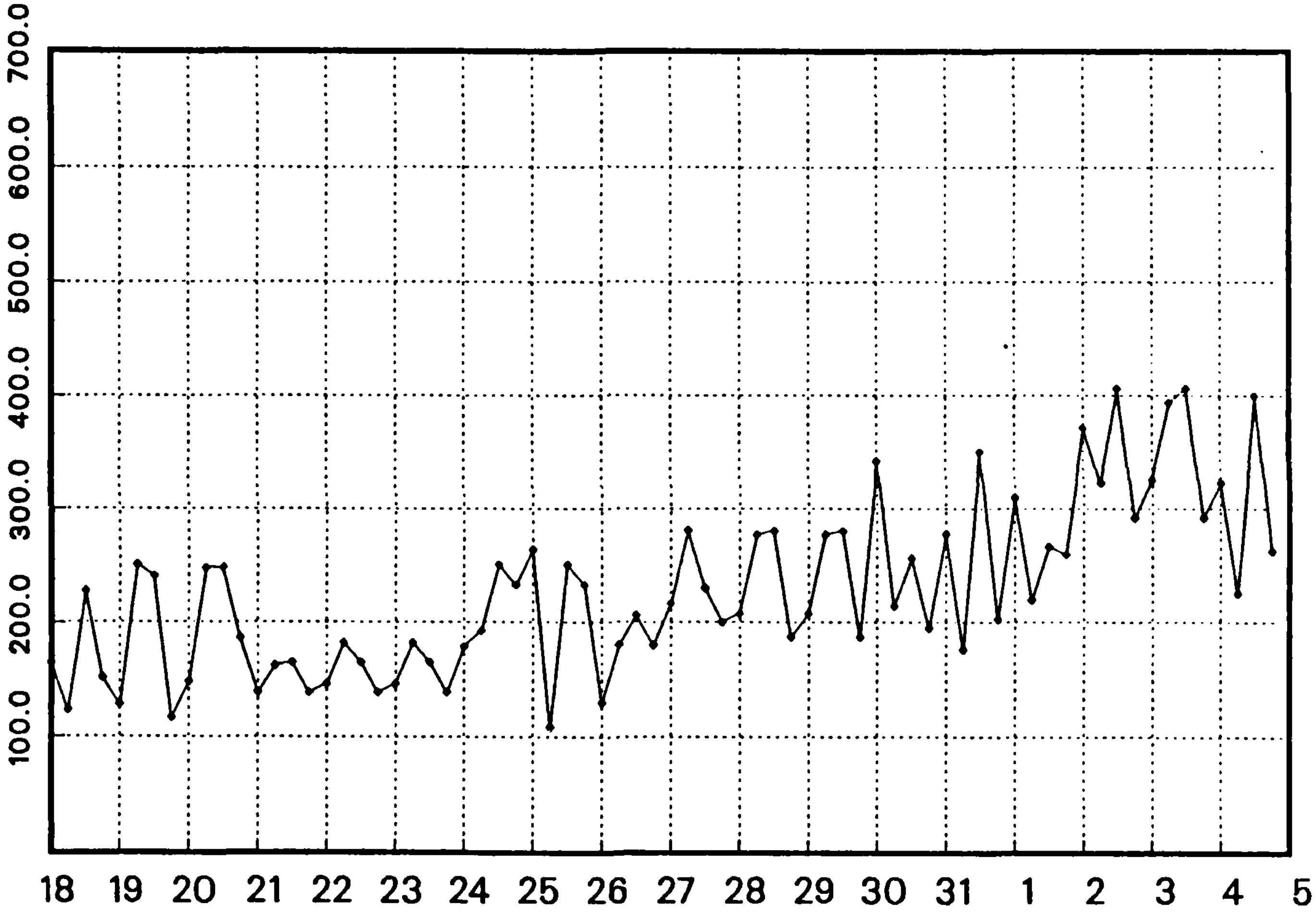

Fig. 2.11. As in Fig. 2.10, except for the NW point.

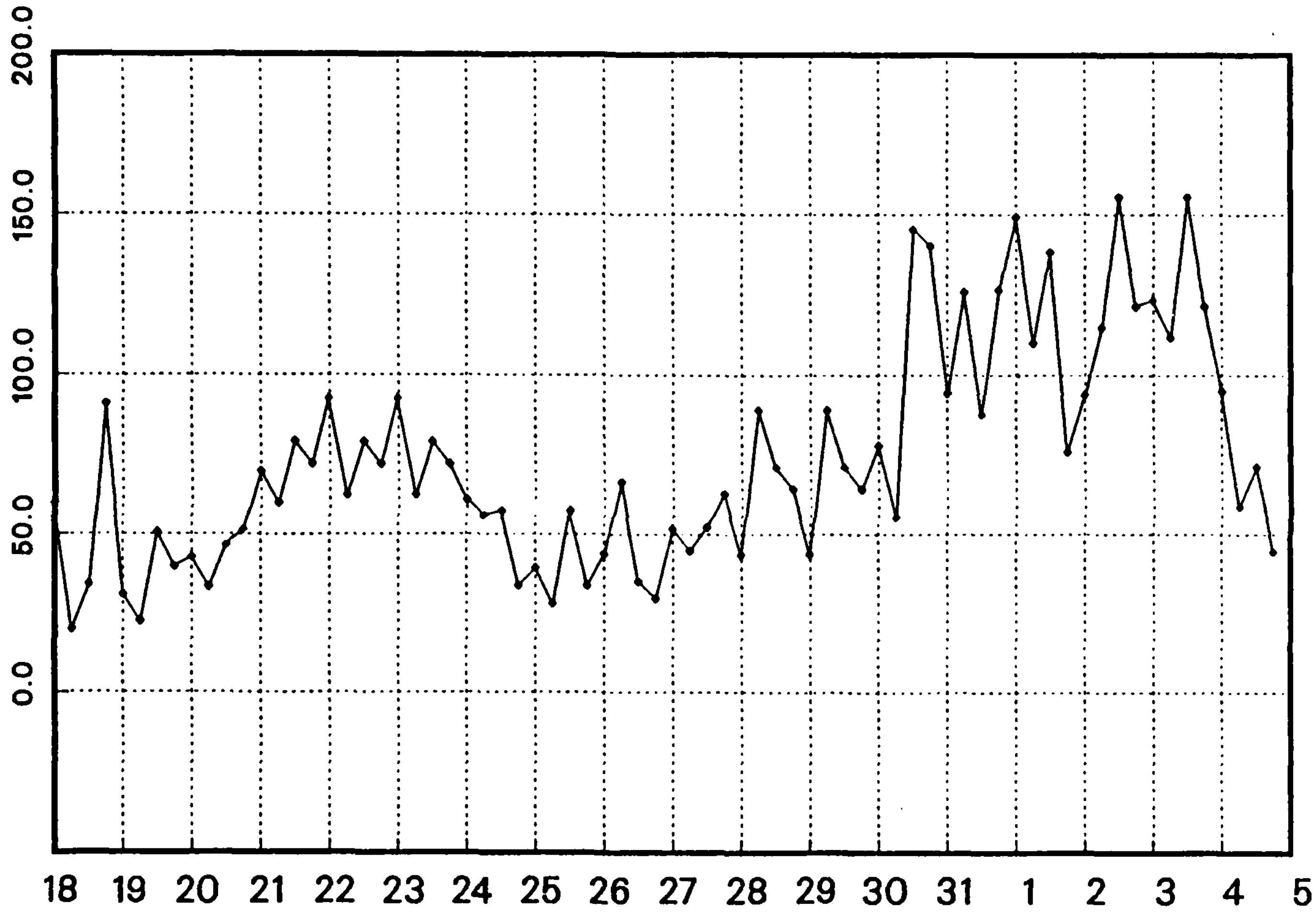

Fig. 2.12. Sensible heat flux (W/m^2) at the SW point during the onset in 1985 (18 May-4 June). Date of onset is ~27 May. Values are plotted every 6 hours.

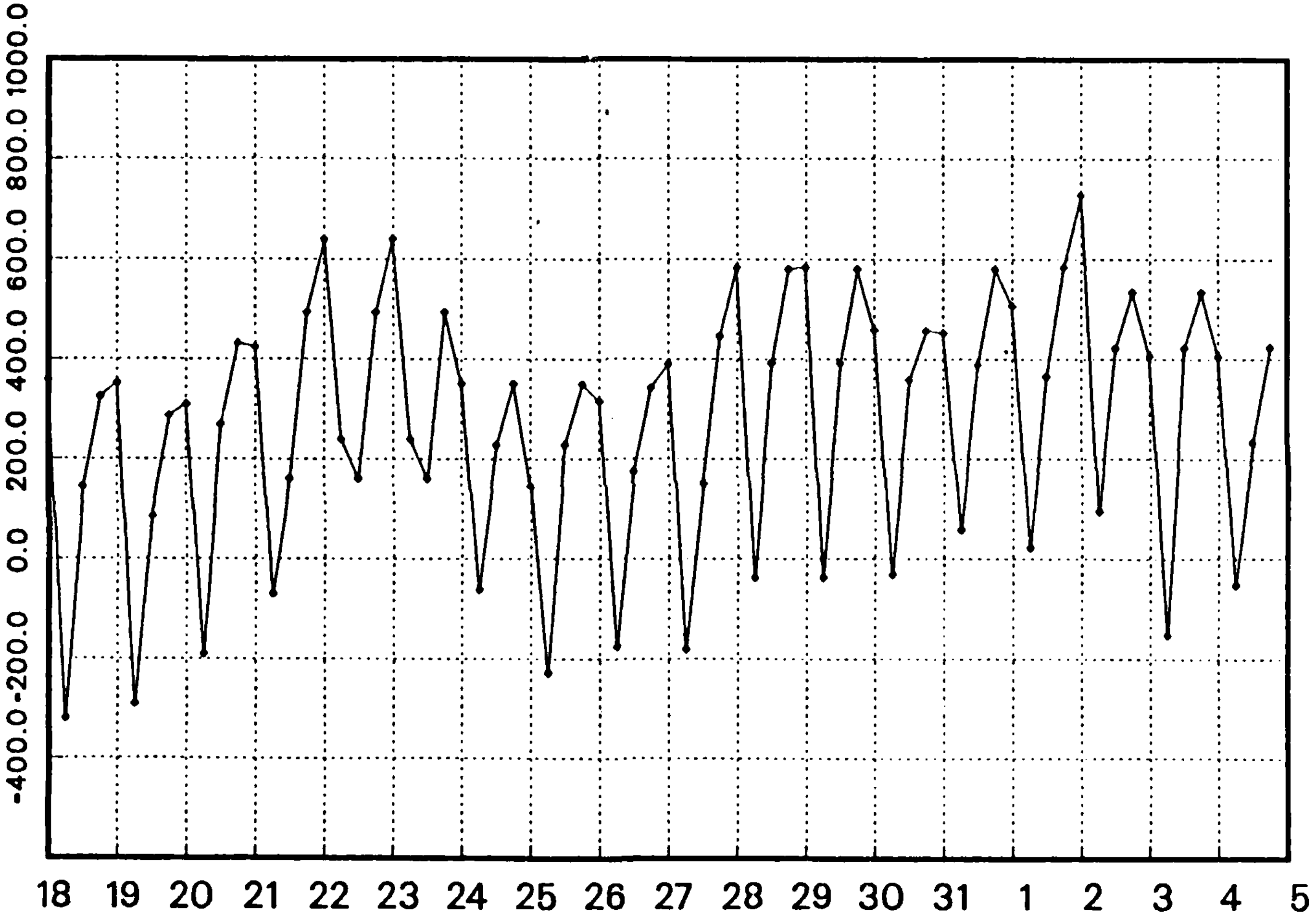

Fig. 2.13. Total (net) surface heat flux (W/m^2) at the SE point during the onset in 1985 (18 May-4 June). Positive values indicate upward heat flux. Date of onset is ~27 May. Values are plotted every 6 hours.

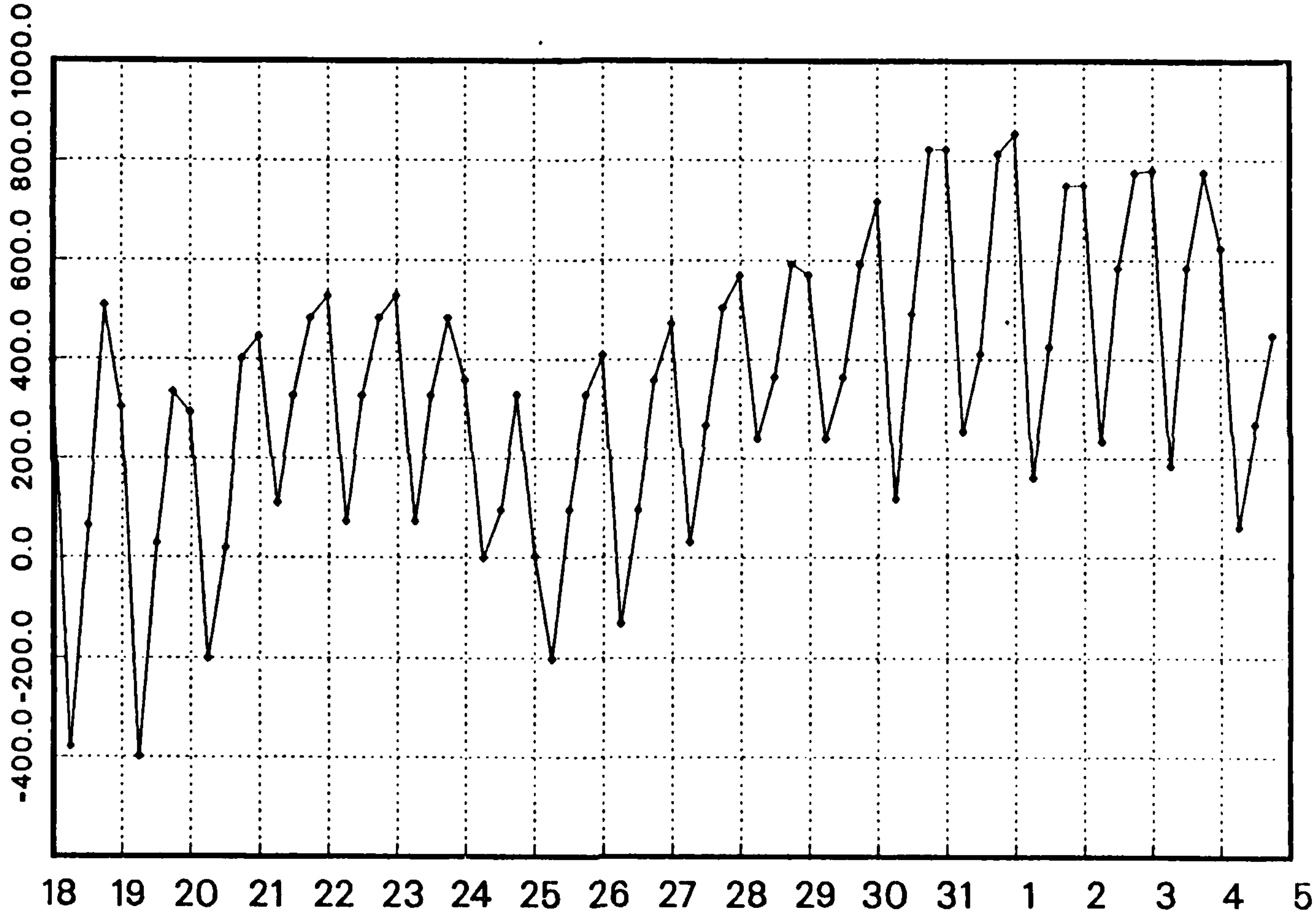

Fig. 2.14. As in Fig. 2.13, except for the SW point.

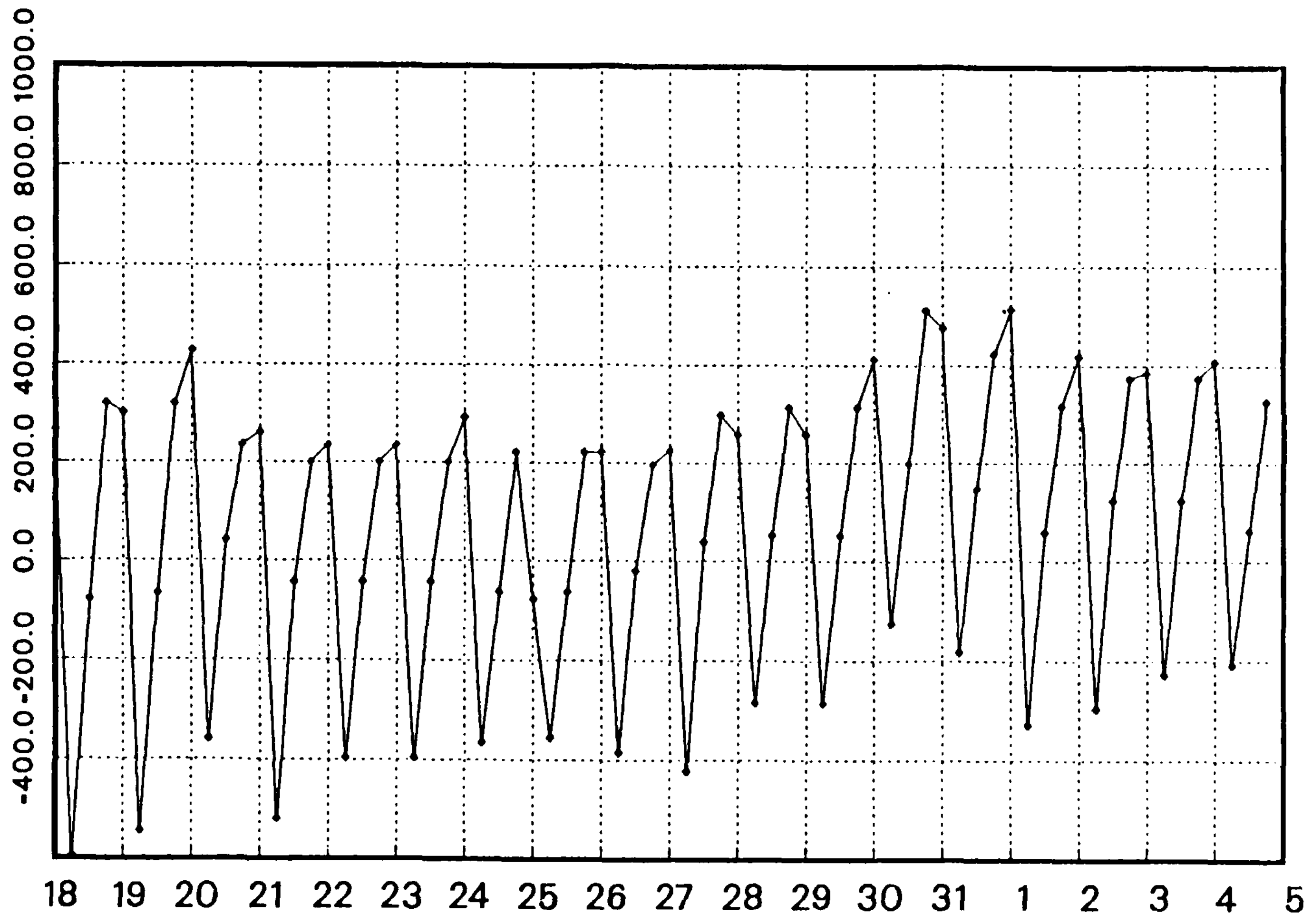

Fig. 2.15. As in Fig. 2.13, except for the NE point.

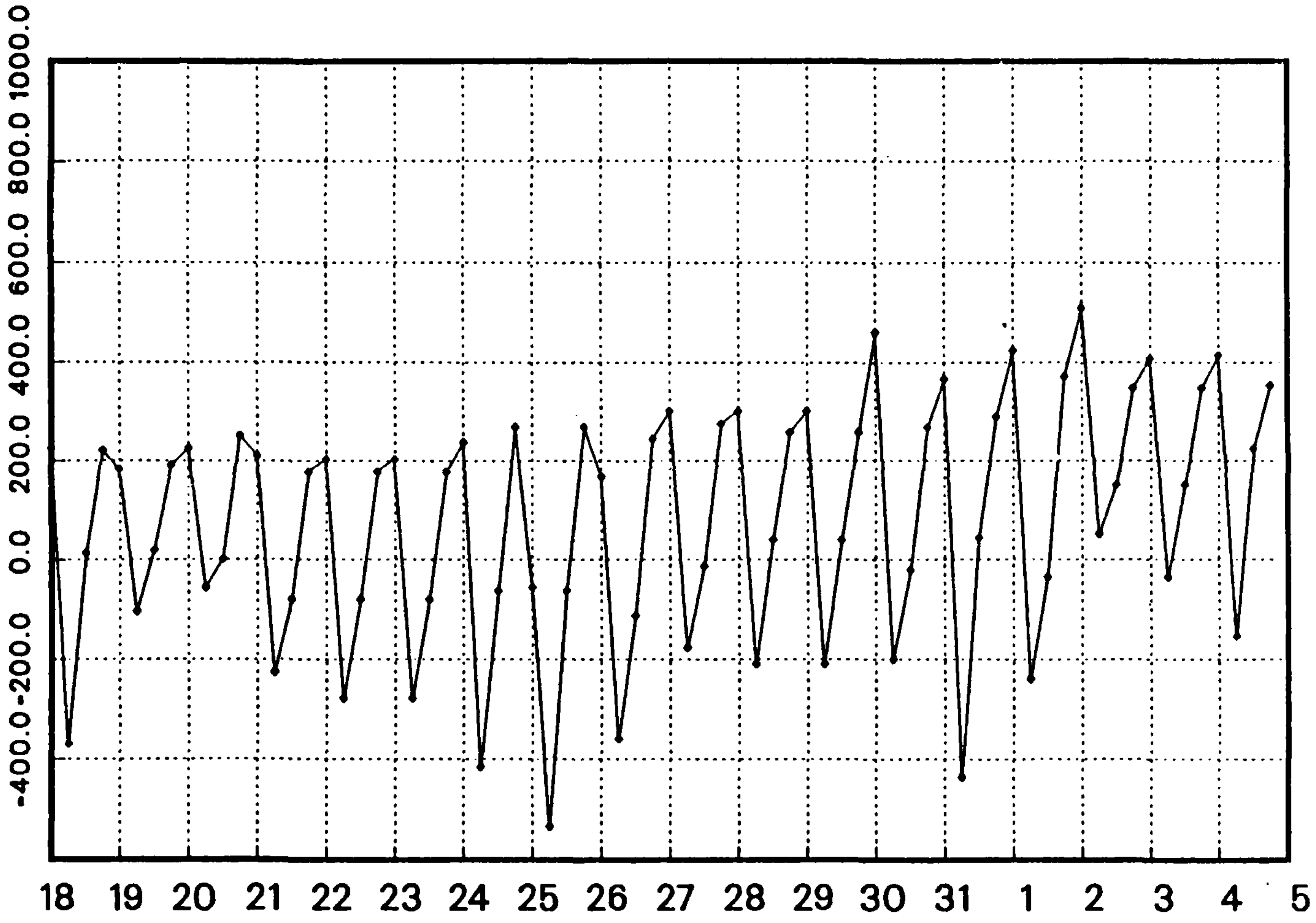

Fig. 2.16. As in Fig. 2.13, except for the NW point.

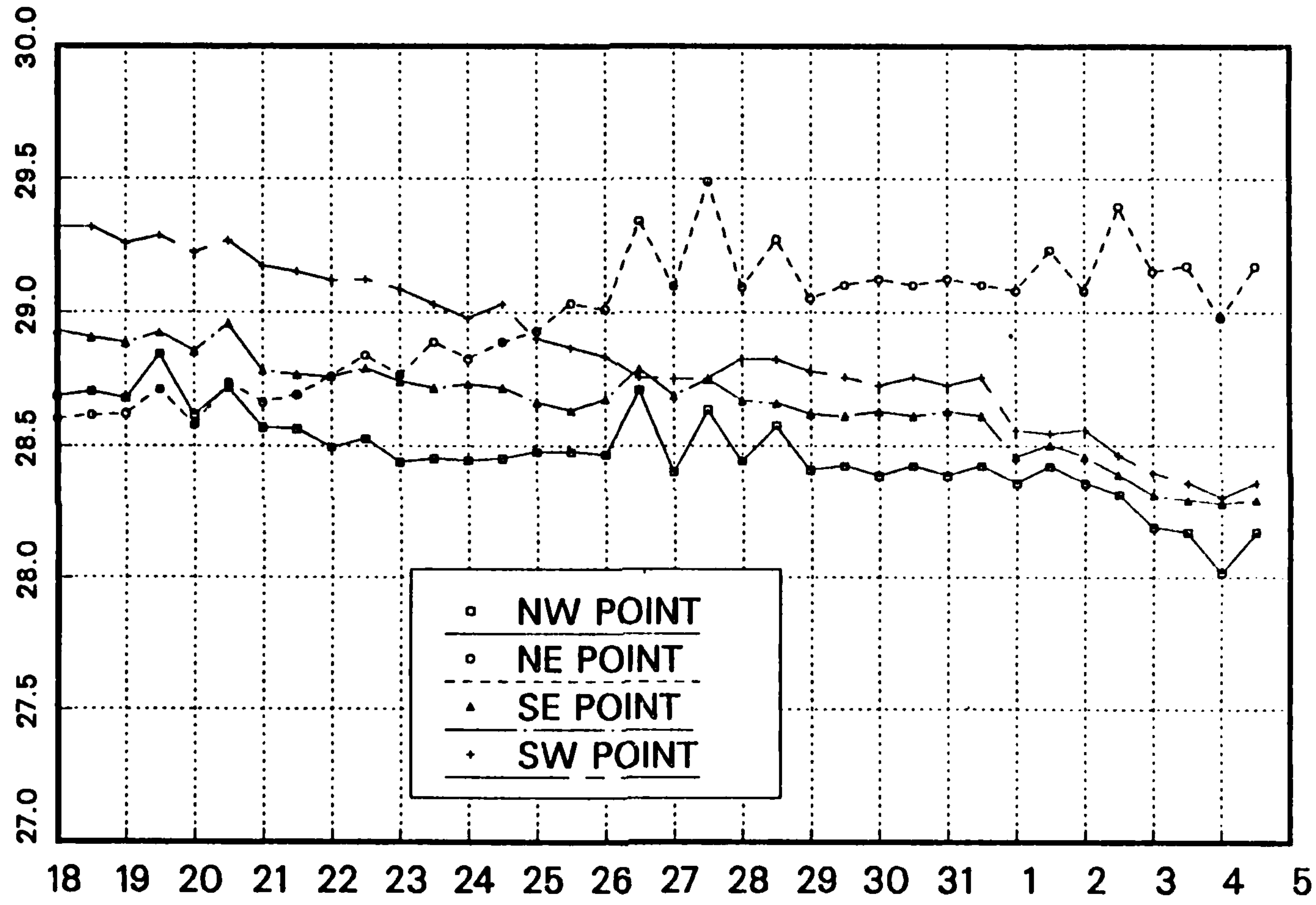

Fig. 2.17. NOGAPS SST (^{o}C) at all points during the onset in 1984 (18 May-4 June). Date of onset is ~27 May. Values are plotted every 12 hours. Solid: NW point; dash: NE point; chain-dot: SE point; Chain-dash: SW point.

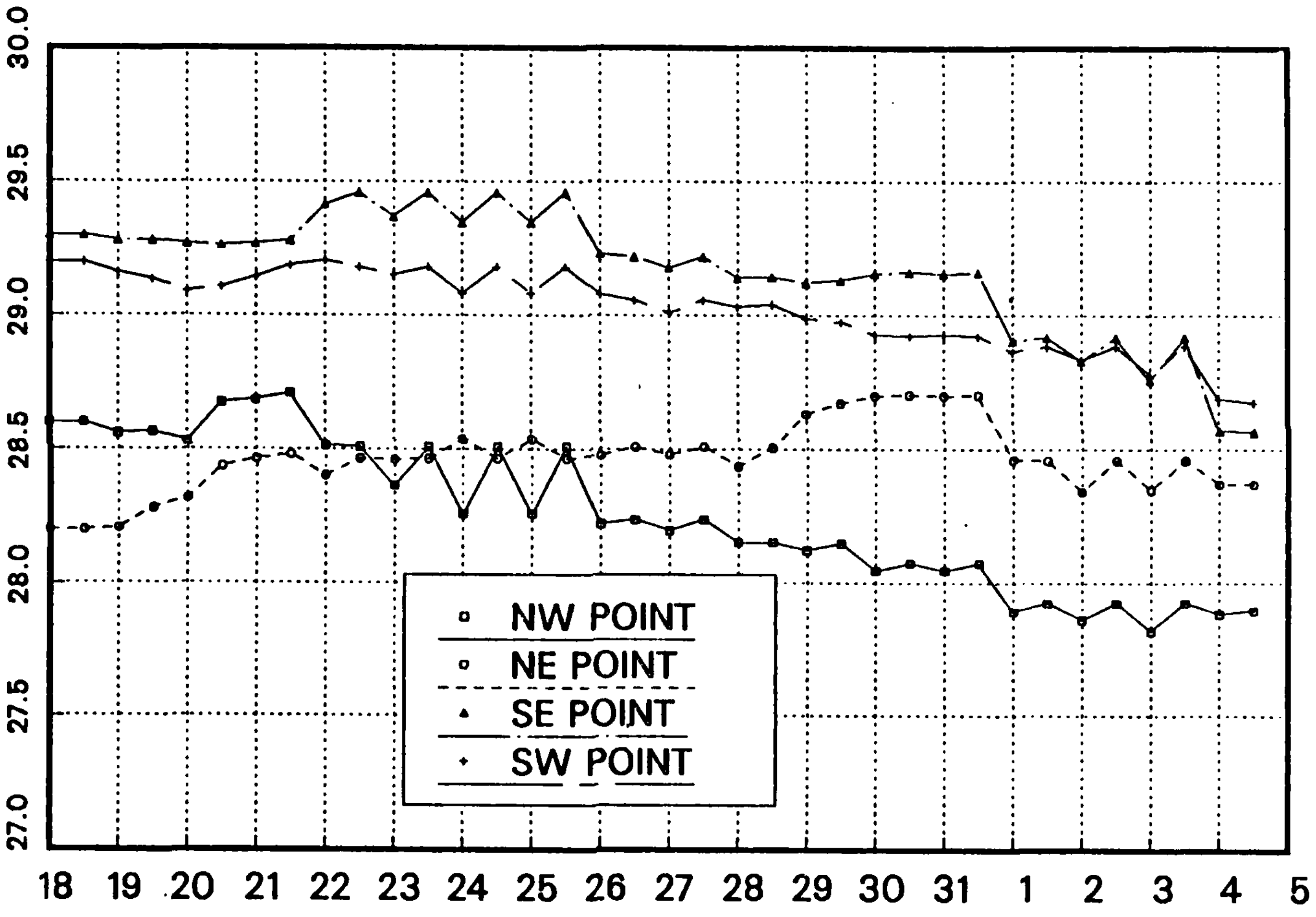

Fig. 2.18. As in Fig. 2.17, except for 1985.

III. *LOCAL FORCING APPLIED TO AN OCEAN MIXED LAYER MODEL*

A. THE MODEL

The ocean mixed layer model (Garwood, 1977) is a one-dimensional, vertically integrated model. Consequently, horizontal and vertical advection are not included in the model. It is only valid for predicting mixed layer conditions on time and space scales where advection can be neglected. It is assumed that the area being studied is far enough from the Somali current and the time scale is small enough (on the order of 5-10 days) that advection is not a significant factor for cooling the mixed layer. The model requires four sets of parameters to predict the response of the mixed layer: the ocean temperature and salinity structure in the upper 200 m; net surface heat flux (Q_n); magnitude of the surface wind stress (τ); and the solar radiative flux (Q_s). The three sets of atmospheric forcing data are obtained directly from the NOGAPS model output. The net heat flux is the sum of evaporative heat flux, sensible heat flux, solar radiative flux and long-wave radiative flux. Q_n is positive for upward heat flux from the ocean to the air. As was discussed in Chapter II, the evaporative and sensible heat fluxes both increase significantly during the monsoon onset. Upward fluxes of these quantities contribute directly to cooling the mixed layer at the surface and to generation of convective turbulence that cools the layer by entrainment at the base of the layer.

The magnitude of the surface wind stress (τ) is computed from the NOGAPS wind speeds using the formulation found in Gill (1982):

$$\tau_x = C_d \rho V u;$$
$$\tau_y = C_d \rho V v;$$
$$\tau = (\tau_x^2 + \tau_y^2)^{1/2},$$

where τ_x is the zonal wind stress; τ_y is the meridional wind stress; C_d is the drag coefficient for the ocean surface; ρ, the density of air, is set to 1.22 kg/m^3; V is the wind speed; and u and v are the zonal and meridional components of the wind speed. For speeds at or below 6 m/s, $C_d = 1.1 \times 10^{-3}$. For speeds greater than 6 m/s, $C_d = (0.61 + 0.063V) \times 10^{-3}$. Wind stress also increases significantly during the monsoon onset and tends to deepen the mixed layer by entrainment of water from below the mixed layer. As the generation of turbulent kinetic energy (TKE) is proportional to the third power of the wind speed, this deepening mechanism is highly variable even after onset.

Wind stress mixing and evaporative heat flux are obviously closely related. However, the sensitivity study can indicate whether the primary heat flux takes place at the surface or at the base of the mixed layer.

As described in Chapter II, the solar radiative flux (Q_S) does not decrease as much as the other two atmospheric forcing mechanisms increase during onset. In the ocean mixed layer model, a fixed fraction of the solar radiation is absorbed in the first meter of the layer and the remainder of the absorption occurs exponentially with depth below one meter (Stringer, 1983). The very strong insolation before onset in the Arabian Sea tends to produce shallowing and warming of the mixed layer. One purpose of this study is to determine how much effect the increased cloudiness associated with onset has on the SST and mixed layer depth. The mixed layer model uses the wind stress and surface heat flux to calculate the TKE and the vertical flux of TKE within the mixed layer. Garwood (1977) indicates that this flux is the major source of mixing within an active entrainment zone at the base of the mixed layer. All of the data are input on an hourly basis. Salinity is held constant with depth because of the lack of observational data. It is set at 35.5 parts per thousand, which agrees with surface isohaline distributions found in Tchernia (1981).

Given the initial structure of the mixed layer and the atmospheric forcing, the model predicts the changes in temperature and mixed layer depth. Wind stress produces TKE which causes mixing and entrainment. However, entrainment offsets the TKE production by entraining colder water with less TKE. The surface buoyancy force can either produce TKE (through convective overturning initiated by surface cooling) or damp TKE (stabilization due to surface heating). If the intensity of the TKE and surface buoyancy force are large enough to overcome the buoyancy force below the base of the mixed layer, the mixed layer will deepen. If the intensity of the TKE or the surface buoyancy forces diminish, the mixed layer will retreat to a shallower equilibrium depth on the order of the Obukhov depth. This depth is where surface heating of the mixed layer is balanced by cooling due to entrainment or upwelling.

The atmospheric forcing terms that have been discussed are applied to this ocean mixed layer model to investigate three questions:

1. How well does the Garwood ocean mixed layer model predict the mixed layer temperature and depth using the atmospheric forcing terms discussed above at low latitudes during the summer months?
2. Does the ocean mixed layer model predict SST changes during onset that compare favorably with the SST values from the NOGAPS analyses?

3. What is the sensitivity of the mixed layer predictions to each of the three atmospheric forcing terms?

The monsoon onsets of 1984 and 1985 are investigated because the atmospheric forcing terms are readily obtainable from NOGAPS. To provide the initial temperature fields in the Indian Ocean, the regional Extended Ocean Thermal Structure (EOTS) analyses for 1984 and 1985 were interpolated to the points illustrated in Fig. 2.1. The regional EOTS objective analysis system (Clancy and Pollak, 1983) integrates all available Expendable Bathythermograph (XBT) data in a given region with climatology. It is run twice a week with all XBT observations since the last run. EOTS produces temperature profiles from the surface to 400 m at 17 fixed levels and at 5 floating levels which are centered about the mixed layer depth. The horizontal domain is a 63 x 63 grid with approximately 50 km grid spacing in the tropics (Ken Pollak, FNOC, personal communication). When XBT observations are not available, the analysis is adjusted toward climatology. A significant problem is the paucity of observations of both atmospheric and oceanic conditions in the Arabian Sea region. In this case, very few ocean temperature profiles are available during the period with the atmospheric forcing data from NOGAPS.

The SST from the EOTS profiles differ in magnitude and trend relative to the NOGAPS model SST analyses described above. For example, the NOGAPS SST analysis indicates a decrease in temperature from 29.1 °C to 28.3°C at the SW point in 1985. The corresponding EOTS SST analysis indicates that the temperature increases from 29.3 °C to 29.5°C. There are two reasons for the differences in SST. First, the two data sets are analyzed on two different grids. The NOGAPS grid spacing is approximately 150 km in the tropics and is much coarser than the EOTS grid. Secondly, the EOTS data indicate no apparent response to the onset forcing fields. Since the onset occurs at a different time each year, the climatological SST analyses tend to average out the response to onset forcing. The EOTS SST analyses appear to be based mostly on climatology. These restrictions prevent a verification study of the ocean thermal structure predictions. Rather, the emphasis will be on the relative sensitivity of the mixed layer predictions to each atmospheric forcing mechanism.

Climatological temperature profiles are derived from Naval Oceanographic Office Reference Publication 42C (1982). These temperature profiles are based on many years of XBT observations during May at each location. The average SST and mixed layer depth are used to construct the mixed layer profile. Given the mixed layer temperature and depth and the temperature at 200 m, the remainder of the temperature profile is given by:

$$T(z) = T_0 \exp[\gamma(z-z_0)], \qquad (3.1)$$

where $T(z)$ is the temperature at depth z; T_0 is the mixed layer temperature; z_0 is the depth of the mixed layer, and $\gamma = \ln[T(200)/T_0]/[200-z_0]$. The temperature at 1 m below the mixed layer depth is set equal to $T_0 - 1$. This exponential profile approximates the climatological profile reasonably well (Fig. 3.1). Thus, the initial temperature profiles are determined by the SST (which is also the mixed layer temperature), the mixed layer depth and the temperature at 200 m, as listed in Table 8.

TABLE 8

Climatological SST, mixed layer depth and temperature at 200m at the four points.

	SE	SW	NW	NE
SST (°C)	29.9	29.3	29.0	31.9
M.L. Depth (m)	40	60	30	30
T200 (°C)	14.2	14.8	15.5	17.2

The shallower mixed layer at the northern two points relative to the two southern points is probably because the axis of the developing low-level jet is closer to the southern points just prior to onset. The SST at the NE point is suspiciously high compared to the climatological isotherm analyses of Tchernia (1981) and the Monthly Oceanography Summary for May 1985. In any case, the initial SST has only a limited effect on the mixed layer model. The simulated mixed layer responds quickly to the atmospheric forcing and an equilibrium thermal structure develops within 4-5 days. The lower SST at the NW point is probably due to the influence of the Somali Current as it spreads over the northern Arabian Sea. The actual SST at the NE point is probably somewhat higher than the SST at the southern points because of the lighter winds.

B. MIXED LAYER PREDICTIONS DERIVED FROM THE ATMOSPHERIC FORCING

The atmospheric forcing fields are applied to the ocean mixed layer model in two phases. First, the FNOC forcing fields during 1984 and 1985 are applied at all four points to determine the mixed layer development and to compare the predicted SST to the NOGAPS analyzed SST. A similar test of the NASA atmospheric forcing during 1979 is not done as no verification data on the evolution of the SST are available to us. Second, pre-onset mean atmospheric forcing values are substituted for the actual data to determine the evolution of the mixed layer temperature and depth in the absence of an onset event. Each forcing mechanism is then examined by selectively substituting the actual forcing values while keeping the other two forcing mechanisms at their pre-onset mean values. The second phase is illustrated for the SE point only during the period 22 May to 6 June 1985. This point is chosen because it is an area with wide variations between the pre-onset and the post-onset atmospheric forcing fields. The integrations are begun on 16 May to ensure that equilibrium has been achieved with five days of pre-onset forcing before the output is examined. The onset of the monsoon was about 26 - 27 May in 1984 and 1985.

The evolution of the mixed layer temperature and depth during the 1985 onset is illustrated in Figs. 3.2 and 3.3, respectively. Daily maximum mixed layer depths are presented, along with the corresponding mixed layer temperature at that time (usually early morning), because the diurnal changes predicted by the mixed layer model cannot be verified. At the SE point, the pre-onset SST is 29.4°C. and the mixed layer depth is 45 m. Beginning on 26 May, the SST decreases steadily to about 28.3°C and the mixed layer deepens to 57 m. As seen in Figs 2.10 and 2.16, this is approximately the date that the net heat flux and wind speed increase in magnitude.

At the SW point, the pre-onset SST is 29.0°C and the mixed layer depth is 62 m. Following monsoon onset, the mixed layer cools by 1.5°C and deepens by 21 m in nine days. This large cooling and deepening at the SW point is even more significant since the initial mixed layer depth was largest at this point.

Prior to onset, the mixed layer at the NW point warms and shallows very rapidly in response to atmospheric forcing. The average mixed layer temperature is 32°C and the mixed layer depth is 3-8 m. Formation of such a warm, shallow layer at the surface is an excessive response in the model to the strong insolation and light winds that exist prior to onset. If the SST was really this high, the surface heat fluxes would be much higher than the NOGAPS atmospheric forcing fields, which are based on actual SST values. That is, a fully coupled ocean-atmosphere model in which the surface fluxes depend on the predicted SST would be more realistic than the procedure used here of prescribing externally the actual atmospheric forcing fields.

There are several possible explanations for the excessive warming and shallowing that is simulated in the mixed layer model. The NOGAPS analysis uses an algorithm to indirectly estimate the cloud cover based on the humidity fields. The algorithm could result in too high values for Q_S which would cause too much warming and shallowing. However, the NOGAPS solar fluxes described above appear to be too small relative to Gautier (1986). The mixed layer model may not use the proper distribution of solar radiation absorption in the mixed layer. If too large a fraction of the Q_S is assumed to be absorbed in the first meter, it would also cause excessive warming and shallowing. There are usually very few wind observations in this area for use in the NOGAPS analysis. Low wind speeds from NOGAPS could also result in a shallow warm layer. As there may be a combination of causes in this case, the answer is unclear. Stringer (1983) reported similar predictions of warm and shallow layers during the spring and summer months in the North Pacific Ocean.

Beginning on 25 May, the mixed layer at the NW point immediately starts cooling and deepening. Although the net temperature difference between 22 May and 6 June is nearly zero, the layer cools by 2.5^{o}C and deepens by 20 m between 25 May and 6 June. During this period the fictitious warm and shallow layer near the surface is eliminated.

The NE point experiences even more excessive warming prior to onset and similar cooling and deepening after onset. The net mixed layer temperature and depth change (positive values represent cooling and deepening) as well as the maximum mixed layer temperature and depth change within the period are listed in Table 9 for all four points. The results for the 1984 onset period show the same tendencies as in 1985.

Simpson and Dickey (1981) examined two classes of parameterization of solar irradiance in various mixed layer models. The first class used a single attenuation length and the other class of models used two attenuation lengths. The models with two attenuation lengths were more sensitive to the surface fluxes and absorbed more solar radiation in the upper few meters. The differences between the two classes of models were greater for light wind conditions, which is the case during the pre-onset period at the northern points. Martin (1985) found that the turbidity also affected the absorptive properties of the mixed layer. These studies indicate that the mixed layer model must be adjusted to the conditions of the atmosphere and ocean if it is to simulate accurately the mixed layer changes. The Garwood mixed layer model uses two attenuation lengths (one of which is very short), and is not adjusted to account for possible variations in the turbidity of the water. The model is tuned for midlatitude solar fluxes, wind speeds and turbidity, and it is not able to simulate accurately the pre-onset mixed layer changes.

TABLE 9

Initial SST and mixed layer depth and resulting cooling (°C) and deepening (m) predicted by the mixed layer model using actual forcing values at the four points in 1984 and 1985. Net value is the difference between the final and initial value. Max value is the difference between the max. and min. values in the period.

YEAR	PT	PRE-ONSET		COOLING		DEEPENING	
		SST	MLD	NET	MAX	NET	MAX
1984	SE	29.5	42	0.4	0.4	6	37
	SW	29.0	63	0.9	0.9	11	11
	NW	30.0	3	0.4	0.3	27	28
	NE	32.4	3	0.2	1.5	28	28
1985	SE	29.0	45	1.1	1.1	11	11
	SW	29.0	62	1.5	1.5	20	27
	NW	31.7	3	0.0	2.5	19	19
	NE	36.7	2	1.8	2.8	10	10

Table 10 lists the values for SST for both the ocean mixed layer model and the NOGAPS analysis for all four points before and after onset in 1985. Only at the SE point do the NOGAPS and mixed layer model results agree. Despite using a similar temperature profile to initialize the mixed layer model, the atmospheric forcing mechanisms at the northern points cause the mixed layer to warm and shallow rapidly during the pre-onset period so that the NOGAPS SST and mixed layer temperatures are quite different when onset begins. For these reasons, this study will analyze the sensitivity of

TABLE 10

Pre-onset and post-onset SST (°C) for the mixed layer model and NOGAPS at the four points in 1985.

	Pre-onset SST		Post-onset SST	
	ML Model	NOGAPS	ML Model	NOGAPS
SE	29.4	29.4	28.3	28.4
SW	29.0	29.2	27.5	28.4
NW	31.7	28.5	31.7	27.7
NE	36.7	28.5	35.0	28.3

the mixed layer predictions to the forcing terms rather than emphasizing the comparison between the mixed layer model SST and the NOGAPS SST.

In Phase 2a, constant values for Q_n, τ and Q_s representing pre-onset conditions are provided to the model. The purpose of this procedure is to establish a baseline for comparing the relative effects of each of the three atmospheric forcing terms. The primary requirement is that the mixed layer be in a relatively steady state while using reasonable values for the forcing terms. If the actual pre-onset values are used, the mixed layer would gradually warm since the strong insolation would not be balanced by the net surface heat losses or by mixing due to wind stress. These pre-onset values are based on the results of the atmospheric forcing analysis presented in Chapter II. However, they have been empirically adjusted to maintain a nearly constant mixed layer temperature and depth throughout the pre-onset period. The values are: Q_n = 135 W/m^2; τ = 0.02 N/m^2, and Q_s = 150 W/m^2. Therefore, the net surface heat flux is approximately 50% larger than the actual pre-onset value and the other forcing terms are representative of the pre-onset values. The resulting mixed layer characteristics are listed in Table 11 .

With this baseline pre-onset structure established, the sensitivity of the mixed layer predictions to each forcing term is tested in Phases 2b-2d (Figs. 3.4 and 3.5). In Phase 2b, the effect of Q_n is tested by inserting actual values, while τ and Q_s are held constant at the pre-onset values. As seen in Table 11, the net surface heat flux has a very significant impact on the cooling and deepening of the layer. Comparing values in Table 11, the actual SST decrease (Fig. 3.4) is 1.1°C and the Q_n term alone accounts for 1.1°C cooling. Q_n also accounts for almost half of the mixed layer deepening that occurs when complete atmospheric forcing is specified.

In Phase 2c, the actual values of surface wind stress are inserted while Q_n and Q_s are held constant at the pre-onset values. The increase in surface wind stress after onset has less effect than did the Q_n forcing. The SST decreases by 0.2°C and the mixed layer deepens by 8 m when actual values for τ are used in the model. Even though the mixed layer deepens nearly as much as it does with the Q_n forcing, the cooling is much less because the larger direct surface cooling after onset is not included. Mechanical mixing and subsequent entrainment alone do not appear to be responsible for most of the cooling of the mixed layer. However, at least half of the deepening can be ascribed to wind mixing.

When actual values for Q_s are used (Phase 2d), the mixed layer warms 0.2°C and deepens 3 m. One would expect Q_s to decrease during onset (Gautier, 1986), but the Q_s values from NOGAPS do not decrease. Thus, the question of the relative effect on the ocean mixed layer of the insolation decrease during monsoon onset can not be addressed with these NOGAPS values.

TABLE 11

As in Table 9, except for 1985 at the SE pt. only: Phase 2a, using all pre-onset forcing values; phase 2b, using actual Q_n forcing; phase 2c, using actual τ forcing; phase 2d, using actual Q_s forcing.

PHASE	YEAR	PT	PRE-ONSET		COOLING		DEEPENING	
			SST	MLD	NET	MAX	NET	MAX
2a	1985	SE	30.0	41	0.0	0.0	1	1
2b	1985	SE	29.6	42	1.1	1.1	9	9
2c	1985	SE	29.9	42	0.2	0.2	8	8
2d	1985	SE	30.0	33	-0.2	-0.2	3	10

In summary, the results of Phase 1 indicate the ocean mixed layer model appears to simulate successfully mixed layer changes during the onset at the SE and SW points. The predictions using the atmospheric forcing at the NW and NE points produce unrealistic SST values when compared to other climatological data. The fault may be with the mixed layer model or with the NOGAPS forcing fields or both. An exact answer can only be found if the forcing fields and the resulting mixed layer profiles are compared to true verification data sets. In Phase 2, the net surface heat flux term has the largest influence in cooling the mixed layer during onset, but the net surface heat flux and the wind stress contribute almost equally to mixed layer deepening. Although the net surface heat flux and wind stress are not independent and cannot be totally separated, the model results suggest that the heat flux at the surface is greater than at the base of the mixed layer. That is, while entrainment causes significant deepening, the water that is entrained does not cool the layer significantly.

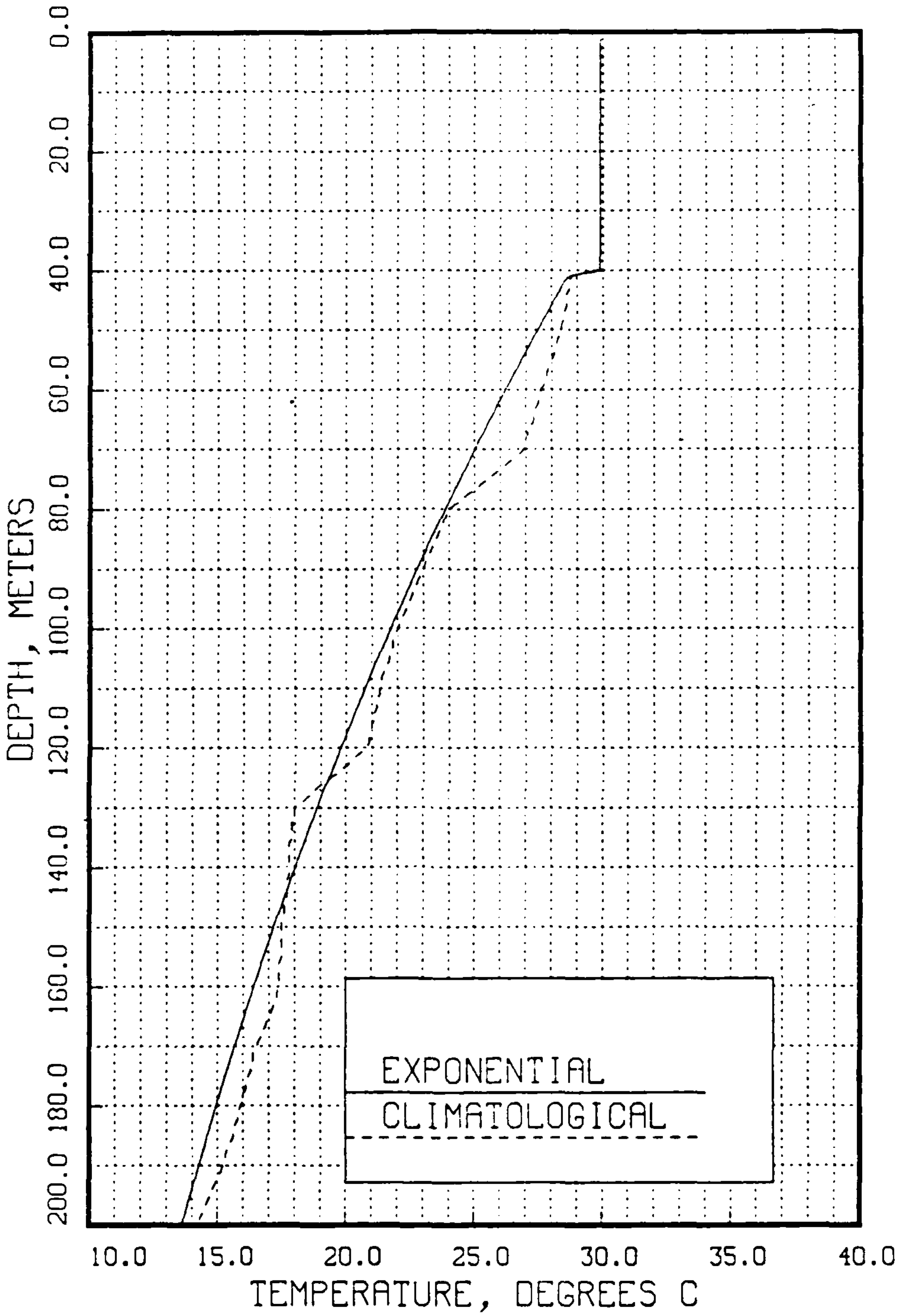

Fig. 3.1. Exponential (solid) approximation of the climatological (dashed) temperature profile at the SE point during May.

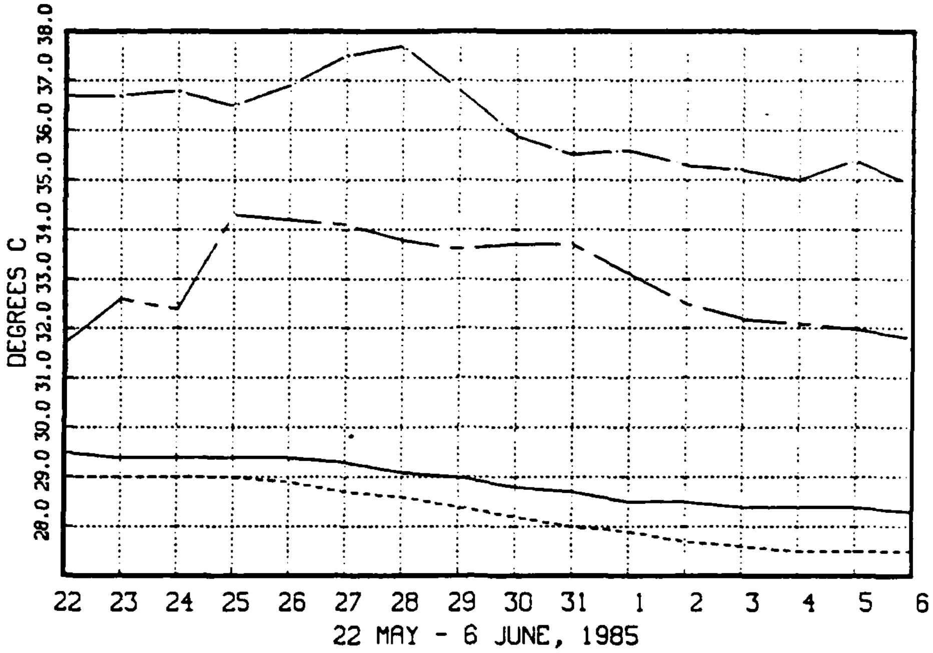

Fig. 3.2. Mixed layer temperature at time of maximum mixed layer depth each day at all points, 1985. Solid - SE point; Dash - SW point; Chain-dot - NW point; Chain-dash - NE point.

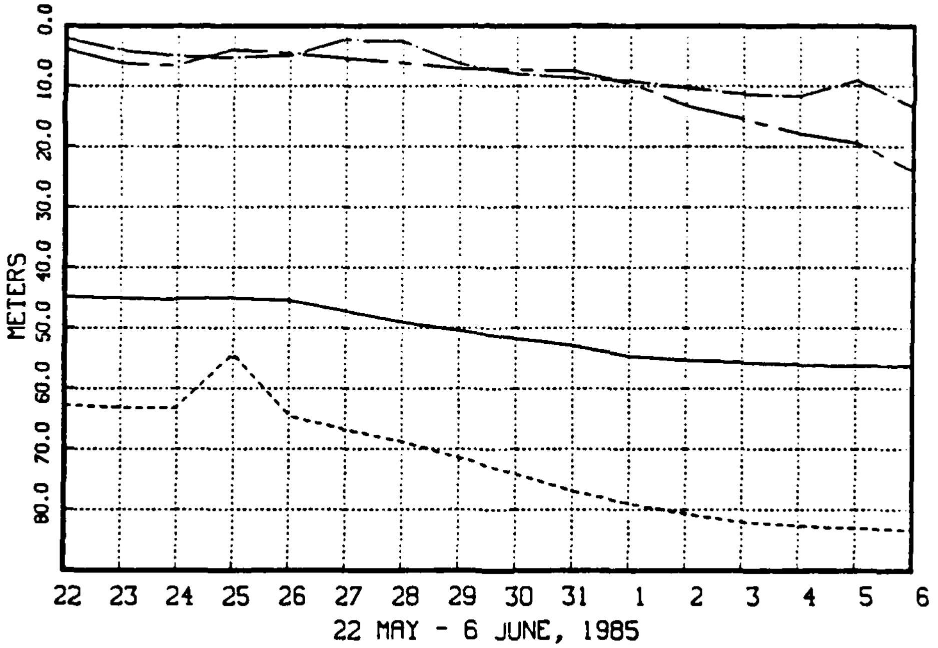

Fig. 3.3. Daily maximum mixed layer depth with 1985 forcing values applied. Same line pattern as in Fig. 3.2.

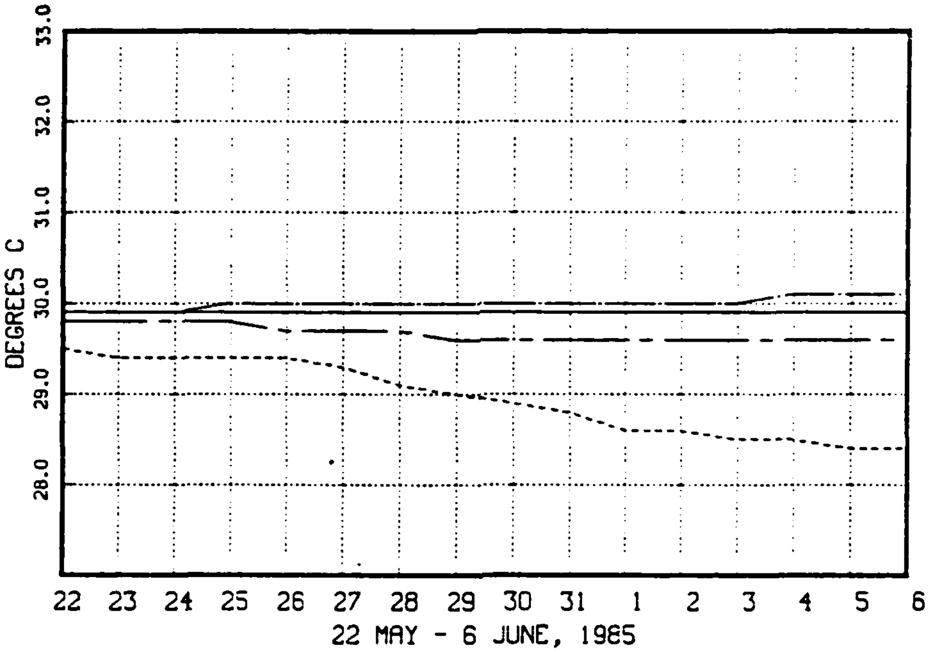

Fig. 3.4. Mixed layer temp. at time of max. mixed layer depth each day with various 1985 post-onset forcing applied. Solid: pre-onset forcing (Phase 2a); dash: Q_n forcing (Phase 2b); chain-dot: τ forcing (Phase 2c); chain-dash: Q_s forcing (phase 2d).

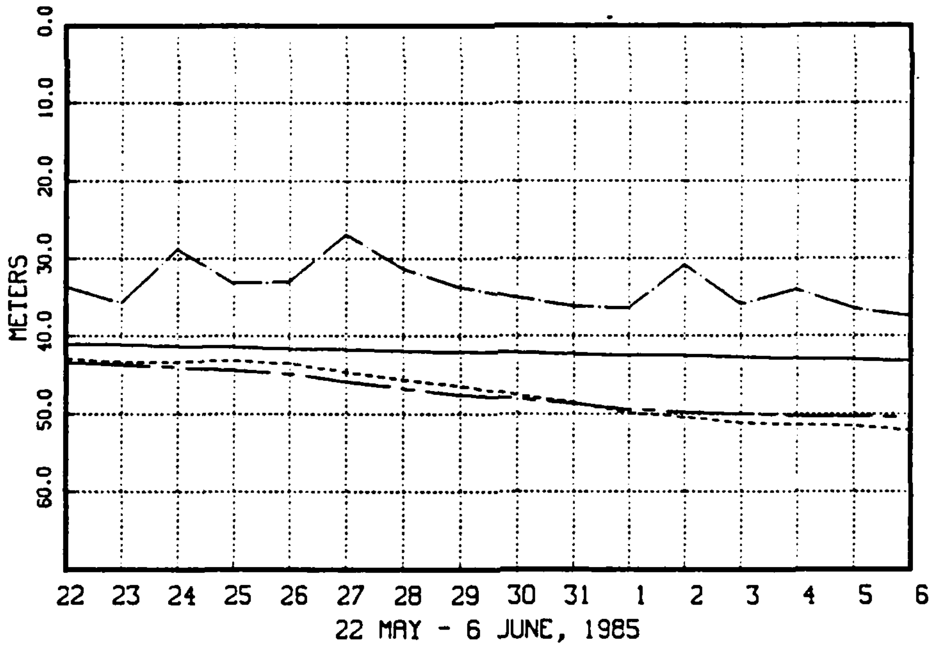

Fig. 3.5. Daily max. mixed layer depths with various 1985 post-onset forcing applied. Same key as in Fig. 3.4.

IV. *CONCLUSIONS*

A. BACKGROUND

The purpose of this study has been to determine the most significant causes for the rapid sea-surface temperature decrease in the Arabian Sea during the onset of the southwest monsoon. The atmospheric forcing of the central Arabian Sea at the time of onset has been examined. Atmospheric forcing data for 1979 are available from the NASA four-dimensional data assimilation model, and data for 1984 and 1985 are taken from the NOGAPS. The forcing fields have been analyzed at four points in the Arabian Sea to determine the pre-onset and post-onset values. The NOGAPS forcing fields are chosen to apply to the Garwood ocean mixed layer model because no SST fields for 1979 are available for verification. The model is initialized with approximations to the climatological temperature and salinity profiles. The model is then run for the period covering the monsoon onset. Phase 1 of this procedure is the application of the actual onset forcing parameters to determine how well the ocean mixed layer could be simulated given these data. Phase 2 involves the application of fixed pre-onset forcing values to the model. The actual onset values of each forcing parameter are then substituted one at a time to test the sensitivity of the mixed layer predictions to each forcing term. The results are also examined in terms of differences among the four points.

B. ATMOSPHERIC FORCING ANALYSIS

The atmospheric forcing fields are evaporative heat flux, wind speed, solar radiative flux and sensible heat flux. The long-wave radiative flux is not examined because it does not change appreciably with the onset and is not expected to contribute to the unusual cooling of the mixed layer. It is important to realize that these forcing terms are not observed quantities, but are the output of a four-dimensional data assimilation system. The NOGAPS analysis has relatively poor observational input in this region and has a coarse grid resolution. Therefore, the atmospheric forcing fields must be utilized with caution.

The solar radiative flux appears to be very dependent upon the algorithm used to estimate it in the atmospheric model. Although the solar radiative flux from the NASA analysis is phase-shifted in time, the total daily heat fluxes are comparable to the NOGAPS solar radiative flux. Whereas Gautier (1986) found a large decrease in insolation over much of the Arabian Sea after the 1979 onset, neither the NASA analysis for 1979 nor the NOGAPS analyses for 1984 and 1985 indicate a significant decrease in solar radiative flux at any of the points. Therefore, the calculations involving solar radiative flux as a possible cause of the mixed layer cooling are inconclusive. The method for calculating this parameter in the NOGAPS analysis should be examined as the potential cause of erroneous ocean predictions in the tropics.

The evaporative heat flux increases dramatically during onset. It is the most significant upward heat flux after onset and it dominates the total (net) surface heat flux. Much of the variation in evaporative heat flux is associated with the changes in wind speed.

The sensible heat flux more than doubles in magnitude after the onset, but it is still significantly smaller than evaporative heat flux and solar radiative flux. It is not believed that the sensible heat flux contributes significantly to the mixed layer cooling during onset.

The final atmospheric forcing mechanism is the wind stress. It is appears to be the most immediate indicator of the monsoon onset over the Arabian Sea. The wind speed dramatically increases as the monsoon begins in all three years. This increase is most obvious near the core of the low-level Somali jet, or to the south of the anticyclonic onset vortex as in 1979. However, it does increase to some extent over the entire Arabian Sea. The increased wind speed has two effects on the ocean mixed layer. First, the increased wind stress generates more turbulence in the mixed layer, which will entrain cooler water from below. Second, the higher wind speed increases the evaporative and sensible heat fluxes. In particular, the wind speed and evaporative heat flux varied in the same manner during the onset period. For this reason, it is difficult to distinguish the relative importance of evaporative heat flux and wind speed.

C. EXAMINATION OF ATMOSPHERIC FORCING WITH THE MIXED LAYER MODEL

Hourly values of the net surface heat flux, surface wind stress and solar radiative flux are derived from the NOGAPS model output for 1984 and 1985 and used as input to a one-dimensional, ocean mixed layer model. The net surface heat flux is the combination of sensible heat flux, solar radiative flux, long-wave radiative flux and evaporative heat flux. Climatological temperature profiles and isohaline salinity profiles are used for the initial mixed layer characteristics as accurate profiles are not available from the operational analyses. The model is initialized on 16 May of both years, which is approximately 11 days before onset, and is run until 6 June, which is approximately 10 days after onset.

At the southern points, the mixed layer model is able to predict SST changes which are close to the NOGAPS SST changes. The SST decrease starts immediately after the first indications of onset based on the atmospheric forcing fields. However, the pre-onset mixed layer temperatures at the northern points are unrealistically high after five days of integration. The solar radiative flux from NOGAPS may be inaccurate or the mixed layer model may not integrate the forcing terms properly under conditions of strong insolation and light winds. More observations are needed to resolve this problem, which severely limits the usefulness of ocean mixed layer predictions in this northern area.

Based on a sensitivity study, the net surface heat flux is the most significant mechanism contributing to mixed layer cooling. When the other forcing terms are fixed at pre-onset values, the post-onset values of the net heat flux account for as much cooling (1.1°C) as when all the forcing terms are set at post-onset values. The net heat flux and the wind stress have nearly equal contributions to the predicted deepening after onset. Increased wind stress alone forces some deepening but only modest cooling of the mixed layer (0.2°C). Since evaporative heat flux is a major part of the net heat flux, the latter is necessarily tied to changes in wind speed (stress). However, the results do imply that heat loss from the sea surface is greater than the downward heat flux at the base of the mixed layer due to entrainment mixing. This suggests that the original hypothesis of this study is must be modified. Both the wind-induced mixing and the evaporative heat flux must be considered to explain the mixed layer cooling and deepening in the Arabian Sea during the monsoon onset.

In summary, this study has only been partially successful in determining the oceanic effects of changes in the atmospheric forcing terms during onset of the southwest monsoon. The conclusion regarding the importance of net surface heat flux must be regarded as tentative because the algorithm used by NOGAPS and NASA to calculate the solar radiative flux may be unsuitable under these southwest monsoon conditions. Given accurate atmospheric forcing, accurate ocean thermal structure observations for verification and a properly adjusted ocean mixed layer model, the study suggests that the ocean mixed layer changes during monsoon onset can be accurately predicted.

This analysis is a useful first step in understanding the cause of the cooling of the Arabian Sea during the monsoon onset. Future studies should use atmospheric forcing based more on observations rather than on model predictions. The data from FGGE best meets this requirement. However, the study should also use concurrent ocean observations for verification of the mixed layer predictions. Once the causes of the Arabian Sea mixed layer cooling are known, then the relationship of this cooling to other monsoon characteristics, such as rainfall, may be more precisely analyzed.

APPENDIX A

THE NAVY OPERATIONAL GLOBAL ATMOSPHERIC PREDICTION SYSTEM

The Navy Operational Global Atmospheric Prediction System (NOGAPS) at the Fleet Numerical Oceanography Center (FNOC) is a slightly modified version of the UCLA general circulation model. NOGAPS has been the Navy's operational atmospheric forecast model since August 1982. The following sections describe the various features of NOGAPS as used during the experiment. This information is adapted from Ranelli (1984). The complete model has been described by Rosmond (1981).

1. DYNAMICS

The dynamics of the UCLA GCM are described in detail by Arakawa and Lamb (1977) and are only discussed briefly here. NOGAPS is a primitive equation model. The prognostic variables are horizontal velocity, V, temperature, T, surface pressure, p_s, and specific humidity, q. Additional prognostic variables associated with the planetary boundary layer (PBL) will be described below. The finite difference scheme has a spatial resolution of 2.4^o lat. by 3.0^o long. The variables are staggered in the horizontal according to the Arakawa scheme C. The center grid point contains the T value. The meridional wind component, v, is carried at points north and south of the center point and the zonal wind component, u, is carried at points east and west of the center point. The numerical differencing scheme is both energy and enstrophy conserving.

NOGAPS uses a sigma coordinate system in the vertical defined as:

$$\sigma = (p - p_i)/\pi$$

where:

$$p_i = 50 \text{ mb and } \pi = p_s - p_i ,$$

p is pressure and p_s is surface pressure. There are six model layers in the vertical with the top of the model atmosphere at 50 mb. All prognostic variables except vertical velocity, σ, are carried at the middle of each layer. Vertical velocity is carried at the layer interfaces.

NOGAPS uses a second order (leapfrog) time differencing scheme with a four minute time step. Model diabatics are executed every forty minutes. A Matsuno time step is used every fifth time step. This is used to control the computational mode and to assist in the assimilation of the diabatic effects.

2. MODEL DIABATICS

The sophisticated model diabatics contained in NOGAPS is an important component in this experiment. This treatment of the diabatic processes is necessary to adequately simulate fluxes across the air-sea interface and to propagate the full effect of these changes throughout the atmosphere. NOGAPS directly computes the physical processes for:

dry convective adjustment
large-scale precipitation
diagnosis of stratus cloud depth
mid-level convection
ground hydrology
surface friction
horizontal diffusion of momentum
radiative transfer processes
cumulus convection

1. *Planetary Boundary Layer*

The planetary boundary layer (PBL) is defined as a well mixed layer in moisture, moist static energy and momentum. It is assumed to be capped by discontinuities in temperature, moisture and momentum. The PBL treatment in this model follows Deardorff (1972) and has been formulated for the UCLA GCM by Randall (1976). It allows for interaction between the PBL and cumulus cloud ensembles and/or a stratus cloud layer at each grid point. Surface fluxes are determined using a bulk Richardson number based on the values of the sea surface temperature and the values of V, T and q from the adiabatic portion of the model. These values are then used to predict a new PBL depth and the strength of the inversion jumps.

The NOGAPS PBL is constrained to remain in the bottom sigma layer of the model. This differs from the original formulation of the UCLA GCM, in which the PBL was allowed to pass out of this layer. An overly deep PBL can result in serious computational problems with the model. Constraining the PBL in this way imposes a maximum depth of about 200 mb on the PBL.

2. *Cumulus Parameterization*

Cumulus parameterization in NOGAPS follows the scheme of Arakawa and Schubert (1974) as introduced into the model by Lord (1978). In the model, cumulus clouds must have their bases at the top of the PBL. Cloud tops can be at all sigma-levels above the PBL. Cumulus clouds are modeled as entraining plumes in which environmental air is mixed with the PBL air from which the cloud originated. Tendencies of moisture, temperature and momentum are diagnosed as well as the cloud mass flux. The cloud base mass flux removes mass from the PBL, which decreases the PBL depth. Condensation occurs at each grid point where the air becomes supersaturated. A moist convective adjustment procedure removes convective instability between mid-tropospheric layers that is not eliminated by clouds originating from the PBL.

3. *Radiation*

The radiation parameterization follows Katayama (1974) and Schlesinger (1976). It includes both a diurnal variation and interaction with the cloud distribution. Radiative transfer processes for incoming solar radiation are computed. Effects of water vapor, Rayleigh scattering by air molecules and absorption and scattering by water droplets in clouds are included. Reflection due to clouds is also calculated. The model cloud cover predicted by the PBL, the cumulus parameterization and large-scale precipitation interact with the long-wave radiation. The net surface heat flux is computed as a function of the incoming solar heat flux, long-wave radiation flux, evaporative heat flux and sensible heat flux.

3. PROBLEMS WITH NOGAPS IN THE TROPICS

The solar radiation flux is computed indirectly from the cloud parameterization calculations and the water vapor distribution. The solar radiation flux analyses in Chapter II indicate that this scheme is not appropriate in the tropical Arabian Sea because the solar radiation flux does not decrease at all after onset. This is not consistent with the findings of Gautier (1986). The NOGAPS parameterization scheme is more appropriate for mid-latitude regions. Therefore, NOGAPS should be used selectively in tropical regions.

APPENDIX B
DATA HANDLING PROCEDURES

1. ATMOSPHERIC FORCING FIELDS

The NOGAPS and NASA atmospheric forcing fields are available at 6-h intervals. The analyses are at 00 and 12 GMT and the 6-h predictions are at 06 and 18 GMT. The NOGAPS atmospheric forcing fields for this study cover the area from the equator to 25°N and from 50°E to 75°E, with 2.5° grid spacing. The NASA atmospheric forcing fields cover the area from 2°S to 26°N in 4° intervals and from 50°E to 75°E in 5° intervals.

The NOGAPS analyses are missing data at all grid points on several days during the onset period. The missing data are replaced with the previous 24-h values of that forcing field at each grid point. This sets the missing value close to the recent trend value instead of setting it to an average value that might be far different from the recent trend.

The data are analyzed in three ways. First, a 10-day average of each atmospheric forcing field at each grid point is computed for the pre-onset period ending 3-4 days before onset. Second, ten-day averages are computed for each atmospheric forcing field for the post-onset period beginning 3-4 days after onset. The pre-onset and post-onset ten-day averages are computed for 00, 06, 12 and 18 GMT, although only the 12 GMT 10-day averages are reported in Chapter II. Finally, a time series of each atmospheric forcing field is analyzed by using a 5-grid point spatial average around each of the four analysis points in Fig. 2.1. The time series begins at 00 GMT approximately eight days prior to onset and continues until 18 GMT approximately ten days after the first day of onset.

2. MIXED LAYER MODEL DATA

The Garwood mixed layer model requires atmospheric forcing input on an hourly basis. This means that the NOGAPS and NASA atmospheric forcing fields must be interpolated since they are analyzed every six hours. As stated in Chapter III, a sophisticated scheme (Gallacher, 1979) is used to interpolate the solar radiation flux fields. The scheme uses the location of the grid point and time of year to estimate the diurnal changes in solar radiation flux. The wind stress and net heat flux are linearly interpolated between the 6-h intervals.

LIST OF REFERENCES

Arakawa, A., and W.H. Schubert, 1974: Interaction of a cumulus cloud ensemble with the large-scale environment, Part I. *J. Atmos. Sci.*, *31*, 674-701.

________, and V.R. Lamb, 1977: Computational design of the basic dynamic process of the UCLA general circulation models. *Methods in Computational Physics*, *17*, Academic Press, 173-265.

Babu, V.R., M.V.Rao and Y. Sadhuram, 1985: Relation between the Arabian Sea surface temperature and monsoon rainfall on the west coast of India. *Tropical Ocean-Atmosphere Newsletter*, May 1985, 2 pp.

Clancy, R.M., and K.D. Pollak, 1983: A real-time synoptic ocean thermal analysis/forecast system. *Prog. Oceanog.*, *12*, 383-424.

Deardorff, J.W., 1972: Parameterization of the planetary boundary layer for use in general circulation models. *Mon. Wea. Rev.*, *100*, 93-106.

Duing, W., and A. Leetmaa, 1980: Arabian Sea cooling: a preliminary report. *J. Phys. Occanogr.*, *10*, 307-312.

Gallacher, P.C., 1979: Preparation of ocean model forcing parameters from FNWC atmospheric analysis and model predictions. Naval Postgraduate School Tech. Rep. NPS 63-79-005, 24 pp.

Garwood, R.W. Jr., 1977: An oceanic mixed layer model capable of simulating cyclic states. *J. Phys. Oceanogr.*, *7*, 455-468.

Gautier, C., 1986: Evolution of the net surface shortwave radiation over the Indian Ocean during Summer MONEX (1979): A satellite description. *Mon. Wea. Rev.*, *114*, 525-533.

Gill, A.E., 1982: *Atmosphere-Ocean Dynamics.* Academic Press, 662 pp.

Katayama, A., 1974: A simplified scheme for computing radiative transfer in the troposphere. Technical Report No. 6. Dept. of Meteorology, UCLA, 77 pp.

Krishnamurti, T.N., 1981: Cooling of the Arabian Sea and the onset-vortex during 1979. Recent progress in Equatorial Oceanography: A Report of the Final Meeting of SCOR Working Group 47 in Venice, Italy, April 27-30, 1981, 1-12.

_______, P. Ardanuy, Y. Ramanathan and R. Pasch, 1981: On the onset vortex of the summer monsoon. *Mon. Wea. Rev.*, *109*, 344-363.

_______, and Y. Ramanathan, 1982: Sensitivity of the monsoon onset to differential heating. *J. Atmos. Sci.*, *39*, 1290-1306.

_______, 1985: Summer Monsoon Experiment - a review. *Mon. Wea. Rev.*, *113*, 1590-1626.

Lord, S.J., 1978: Development and observational verification of a cumulus cloud parameterization. Ph.D. Thesis, Dept. of Atmos. Sci., UCLA, 185 pp.

Martin, P.J., 1985: Simulation of the mixed layer at OWS November and Papa with several models. *J. Geophys. Res.*, *90*, 903-916.

Muller, P., R.W. Garwood Jr. and J.P. Garner, 1984: Effect of vertical advection on the dynamics of the oceanic surface mixed layer. *Annales Geophysicae*, *2*, 387-398.

Naval Oceanographic Office, 1982: Typical Expendable Bathythermograph (TXBT) Data Base, Indian Ocean. Naval Oceanographic Office Reference Publication-42C, 240 pp.

Oceanographic Monthly Summary, *V*, *3*, National Oceanic and Atmospheric Administration, 4 pp.

Pearce, R.P., and U.C. Mohanty, 1984: Onsets of the Asian summer monsoon 1979-1982. *J. Atmos. Sci.*, *41*, 1620-1639.

Ramanadham R., S.V.S. Somanadham and R.R. Rao, 1981: The energy budget at selected stations over north Indian Ocean during MONSOON-77. *Monsoon Dynamics*, Edited by James Lighthill and R. Pearce, Cambridge University Press, 509-521.

Randall, D.A., 1976: The interaction of the planetary boundary layer with large-scale circulations. Ph.D. Thesis, Dept. of Atmos. Sci., UCLA, 204 pp.

Ranelli, P.H., 1984: Response of an atmospheric prediction model to time-dependent sea-surface temperatures. M.S. Thesis, Naval Postgraduate School, 98 pp.

Rao R.R., P.G.K. Murthy, M.G. Joseph and K.V.S. Raman, 1981: On the space-time variability of ocean surface mixed layer characteristics of the central and eastern Arabian Sea during MONSOON-77. Proceedings of International Conference on Early Results of FGGE and Large Scale Experiments, Tallahassee, U.S.A., 20-27.

________, 1984: A case on the influence of summer monsoonal vortex on the thermal structure of the upper central Arabian Sea during the onset phase of MONEX-79, *Deep Sea Research*, *31*, 1511-1521.

Rosmond, T.E., 1981: NOGAPS: Navy Operational Global Atmospheric Prediction System. *Preprints, Fifth Conf. on Numerical Weather Prediction*, Monterey, CA, 74-79.

Schlesinger, M.E., 1976: A numerical simulation of the general circulation of atmospheric ozone. Ph.D. Thesis, Dept. of Atmos. Sci., UCLA.

Simpson, J.J., and T.D. Dickey, 1981: The relationship between downward irradiance and upper ocean structure. *J. Phys. Oceanogr.*, *11*, 309-323.

Stringer, G.L., 1983: One-dimensional model hindcasts of cold anomalies in the North Pacific Ocean. M.S. Thesis, Naval Postgraduate School, 136 pp.

Tchernia, P.: *Descriptive Regional Oceanography*. Pergamon Press, 262 pp.

INITIAL DISTRIBUTION LIST

		No. Copies
1.	Defense Technical Information Center Cameron Station Alexandria, VA 22304-6145	2
2.	Library, Code 0142 Naval Postgraduate School Monterey, CA 93943-5000	2
3.	Chairman Code 63Rd Department of Meteorology Naval Postgraduate School Monterey, CA 93943-5000	1
4.	Chairman Code 68Mr Department of Oceanography Naval Postgraduate School Monterey, CA 93943-5000	1
5.	Professor R. Elsberry Code 63Es Department of Meteorology Naval Postgraduate School Monterey, CA 93943-5000	4
6.	Professor R.W. Garwood, Jr. Code 68Gd Department of Oceanography Naval Postgraduate School Monterey, CA 93943-5000	1
7.	Mr. P. Gallacher Code 68Ga Department of Oceanography Naval Postgraduate School Monterey, CA 93943-5000	1
8.	Dr. T.N. Krishnamurti Department of Meteorology Florida State University Tallahassee FL 32306	1
9.	Dr. C. Gautier Scripps Institute of Oceanography University of California, San Diego La Jolla, CA 92093	1
10.	Mr. Robert Rosenberg Code 611 Manager of Diagnostics Goddard Space Flight Center Greenbelt, MD 20771	1
11.	LT David W. Gillard 1269 Nash Avenue Elyria, OH 44035	2
12.	Director Naval Oceanography Division Naval Observatory 34th and Massachusetts Avenue NW Washington, DC 20390	1

13. Commander 1
Naval Oceanography Command
NSTL Station
Bay St. Louis, MS 39522

14. Commanding Officer 1
Naval Oceanographic Office
NSTL Station
Bay St. Louis, MS 39522

15. Commanding Officer 1
Fleet Numerical Oceanography Center
Monterey, CA 93943

16. Commanding Officer 1
Naval Ocean Research and Development Activity
NSTL Station
Bay St. Louis, MS 39522

17. Commanding Officer 1
Naval Environmental Prediction Research Facility
Monterey, CA 93943

18. Chairman, Oceanography Department 1
U.S. Naval Academy
Annapolis, MD 21402

19. Chief of Naval Research 1
Naval Ocean Research and Development Activity
800 N. Quincy Street
Arlington, VA 22217

20. Office of Naval Research (Code 420) 1
Naval Ocean Research and Development Activity
800 N. Quincy Street
Arlington, VA 22217

21. Scientific Liason Office 1
Office of Naval Research
Scripps Institution of Oceanography
La Jolla, CA 92037

22. Commander 1
Oceanographic Systems Pacific
Box 1390
Pearl Harbor, HI 96860

23. Commanding Officer 1
Naval Eastern Oceanography Center
Naval Air Station
Norfolk, VA 23511

24. Commanding Officer 1
Naval Western Oceanography Center
Box 113
Pearl Harbor, HI 96860

25. Commanding Officer 1
Naval Oceanography Command Center, Rota
Box 31
FPO San Francisco, CA 09540

26. Commanding Officer 1
Naval Oceanography Command Center, Guam
Box 12
FPO San Francisco, CA 96630

END

11-86

DTIC